

Cite this: *J. Mater. Chem. B*, 2025, 13, 1212

## Non-Ti MXenes: new biocompatible and biodegradable candidates for biomedical applications

Vijayakumar G Gayathri,<sup>a</sup> Bartholomew Richard,<sup>b</sup> Jithin Thomas Chacko,<sup>b</sup> Jagadeesh Bayry<sup>a</sup> and P Abdul Rasheed<sup>\*ab</sup>

MXenes are a class of two-dimensional nanomaterials with the general formula  $M_{n+1}X_nT_x$ , where M denotes a transition metal, X denotes either carbon or nitrogen and  $T_x$  refers to surface terminations, such as  $-OH$ ,  $-O$ ,  $-F$  or  $-Cl$ . The unique properties of MXenes, including their tunable surface chemistry and high surface area-to-volume ratio, make them promising candidates for various biomedical applications, such as targeted drug delivery, photothermal therapy and so on. Among the family of MXenes, titanium (Ti)-based MXenes, especially  $Ti_3C_2T_x$ , have been extensively explored for biomedical applications. However, despite their potential, Ti-based MXenes have shown some limitations, such as low biocompatibility. Recent studies have also indicated that Ti MXenes may disrupt spermatogenesis and accumulate in the uterus. Non-Ti MXenes are emerging as promising alternatives to Ti-based MXenes due to their superior biodegradability and enhanced biocompatibility. Recently, non-Ti MXenes have been explored for a range of biomedical applications, including drug delivery, photothermal therapy, chemodynamic therapy and sonodynamic therapy. In addition, some non-Ti MXenes exhibit enzyme-mimicking activity, such as superoxide dismutase and peroxidase-like functions, which play a major role in scavenging reactive oxygen species (ROS). This review discusses the properties of non-Ti MXenes, such as biocompatibility, biodegradability, antibacterial activity, and neuroprotective effects, highlighting their potential in various biomedical applications. These properties can be leveraged to mitigate oxidative stress and develop safe and innovative strategies for managing chronic diseases. This review provides a comprehensive analysis of the various biomedical applications of non-Ti MXenes, including their use in drug delivery and combinatorial therapies and as nanozymes for sensing and therapeutic purposes. The theranostic applications of non-Ti MXenes are also discussed. Finally, the antibacterial properties of non-Ti MXenes and the proposed mechanisms are discussed. The review concludes with a summary of the key findings and future perspectives. In short, this review provides a thorough analysis of the biomedical applications of non-Ti MXenes, emphasizing their unique properties, potential opportunities and challenges in the field.

Received 23rd August 2024,  
Accepted 1st December 2024

DOI: 10.1039/d4tb01904k

rsc.li/materials-b

### 1. Introduction

The advent of two-dimensional (2D) materials has sparked a revolution in several scientific and technological domains. Among these, MXenes, a class of transition metal carbides, nitrides, and carbonitrides, have attracted significant interest because of their unique properties and wide range of potential applications. The general formula for MXenes is  $M_{n+1}X_nT_x$  ( $n = 1-4$ ), where M represents an early transition metal (such

as Sc, Y, Ti, Zr, Hf, V, Nb, Ta, Cr, Mo and W), X denotes carbon and/or nitrogen, and  $T_x$  refers to surface terminations (such as O, OH, F, or Cl), which vary depending on the synthetic process.<sup>1</sup> To date, more than 40 different varieties of MXenes with various chemical orderings and compositions have been synthesized experimentally, while over 100 forms have been predicted theoretically.<sup>2</sup> Compared to other traditional 2D materials, such as graphene, MXenes possess several additional interesting characteristics. These include a wide range of surface chemistries and chemical compositions, superior hydrophilicity, tunable electronic conductivity (ranging from semiconductor to metallic), and broad optical absorption properties.<sup>3</sup> These features make MXenes highly versatile candidates for various applications, such as energy storage, electronics, catalysis, sensing, and biomedicine.<sup>4-6</sup>

<sup>a</sup> Department of Biological Sciences and Engineering, Indian Institute of Technology Palakkad, Palakkad, Kerala, 678 557, India. E-mail: abdulrasheed@iitpkd.ac.in<sup>b</sup> Department of Chemistry, Indian Institute of Technology Palakkad, Palakkad, Kerala, 678 557, India

### 1.1. Synthesis of MXene

Eliminating the Al element by etching using hydrofluoric acid (HF) is the first and most used synthetic method for synthesizing MXene from its parent MAX phase.<sup>7</sup> Because HF is toxic, this method of producing MXene is extremely dangerous. According to studies by Feng *et al.*<sup>8</sup> and Wang *et al.*,<sup>9</sup> the multilayer MXene created by HF etching usually features large structural defects and small lateral diameters. It has been proposed that improved processes that make use of a bifluoride etching solution or mixed lithium fluoride–hydrochloric acid (LiF–HCl) can be used to create MXene with a better lateral size and fewer defects.<sup>10,11</sup>

Several other methods for manufacturing MXene have been developed since its discovery, including molten salt etching, wet chemical etching, chemical vapour deposition (CVD), and electrochemical etching.<sup>12–14</sup> In the molten salt etching process, MXene can be synthesized by etching at high temperatures using Lewis's acids, Lewis-base salts, and fluoride salts.<sup>15</sup> Kim and colleagues effectively produced the  $Ti_3C_2T_x$  MXene by removing Al from the  $Ti_3AlC_2$  MAX phase using LiF/HCl solutions throughout the MXene synthesis process.<sup>16</sup> Li *et al.* successfully synthesized  $Ti_3C_2Cl_2$  and  $Ti_2CCl_2$  MXene by delaminating  $Ti_3ZnC_2$  and  $Ti_2ZnC$  in molten  $ZnCl_2$  using Molten salt etching.<sup>12</sup> This process results in an MXene surface with –Cl functional groups and is more resistant to oxidation than the surface with –F functional groups.

The MXene created by CVD provides large surfaces and outstanding stability, and the lack of terminations makes it easier to investigate its special qualities. Wang *et al.* employed the CVD method to synthesize  $Ti_2CCl_2$  MXene by the reaction of methane and titanium tetrachloride on a titanium surface.<sup>17</sup> Another efficient way to produce MXene is *via* electrochemical etching, which offers more control over process parameters and is an environmentally benign option.<sup>18</sup> The creation of carbon generated from carbide and excessive etching must be avoided by carefully adjusting the etching settings. Through electrochemical etching in an HCl solution at 0.6 V for 120 hours, Sun *et al.* successfully produced  $Ti_2CT_x$ .<sup>14</sup> Additionally, the electrochemical *in situ* synthesis of MXene on electrode surfaces presents a simple and eco-friendly method for fabricating MXene devices and offers clear benefits for electrocatalytic applications. As a proof-of-concept, Li *et al.* synthesized  $V_2CT_x$  electrochemically by modifying the MAX phase material on the cathode and an etchant-containing electrolyte to fabricate an MXene battery.<sup>19</sup> The developed MXene battery exhibited outstanding cycling stability and rate performance. In conclusion, chemically exfoliated MXene has a smaller surface area and the least oxidation stability than mechanically exfoliated MXene. In addition, mechanical exfoliation is a more environmentally friendly method than chemical exfoliation methods.

## 2. Biomedical applications of MXenes

In comparison with other 2D materials, MXenes possess high biocompatibility, with minimal cytotoxicity and immunogenicity,

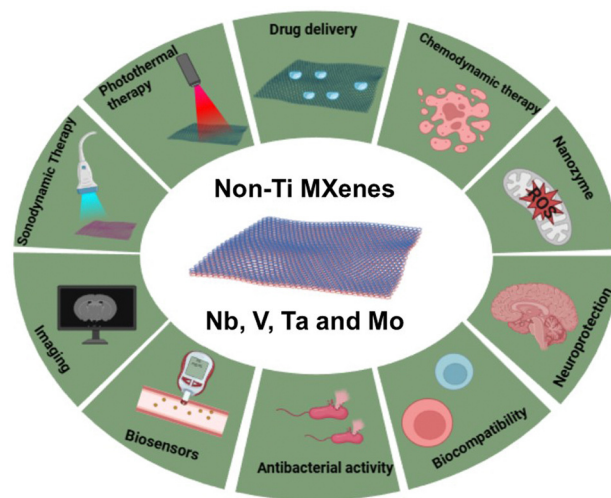


Fig. 1 Biomedical applications of non-Ti MXenes (created with Bio-Render.com).

adaptable surface chemistry and high loading capacity that make them appropriate for various applications in the field of biomedicine, including drug delivery systems, biosensors, antibacterial applications, and various therapies, like photothermal and sonodynamic therapies.<sup>20–24</sup> The schematic showing the various biomedical applications of non-Ti MXenes is illustrated in Fig. 1. The adaptable surface chemistry and high loading capacity make it a valuable component of drug delivery systems, and controlled drug release kinetics can be accomplished by functionalizing MXene with certain compounds.<sup>6,25</sup> MXene-based drug carriers have demonstrated promise in precise drug delivery, with fewer side effects and higher therapeutic efficacy for antibiotics and anticancer drugs.<sup>22</sup> MXenes provide tunable surface functionalities that enable personalised interactions with biomolecules, which in turn make specialised targeting and distribution of drugs with enhancement in their effectiveness.<sup>26–28</sup>

The electrical conductivity and absorption in the near-infrared (NIR) region of MXene-based materials make them a suitable candidate for photothermal therapy (PTT) in the first or second NIR (NIR-I/II) bio window.<sup>29–31</sup> MXenes can produce reactive oxygen species (ROS) under photonic or ultrasonic irradiation because of their configurable bandgap and surface plasmon resonance (SPR) effects. MXenes with multiple defects and a smaller size have been shown to have luminous characteristics and are used in biosensors and molecular imaging.<sup>3</sup> The wide surface area and adjustable surface chemistry of MXenes are ideal for immobilising enzymes, antibodies, and DNA probes to improve target analyte interaction and detection in biosensing applications. Along with the high electrical conductivity and electrochemical activity of MXenes, these properties enable their use in electrochemical biosensing applications.<sup>32</sup> MXene's strong light–matter interactions and SPR make them suitable for optical biosensing.<sup>33</sup> Functionalizing MXene with fluorophores or quantum dots (QDs) creates



optical biosensors that can rapidly and precisely detect real-time biomolecular interactions in a multiplexed manner with high sensitivity.<sup>34–36</sup> Additionally, MXene shows X-ray attenuation and MRI contrast enhancement properties that have significant implications for diagnostic and medical imaging applications, such as CT and MRI contrast agents.<sup>37,38</sup>

MXene shows the capacity to enhance cell adhesion and proliferation and can be utilized in regenerative medicine applications.<sup>39</sup> MXene-based scaffolds have proven to be effective in encouraging cell division, which qualifies them for use in tissue regeneration and repair. These MXene composites can be used in wound healing and organ regeneration by mimicking the extracellular matrix and fostering environments that are conducive to tissue regeneration.<sup>40</sup> In addition, MXene possesses exceptional mechanical strength and flexibility that allow it to tolerate mechanical loads while preserving structural integrity that might be useful in tissue engineering applications.<sup>41</sup>

MXene-based materials have demonstrated the ability to inhibit bacterial growth, making them promising candidates for use as antibacterial agents. This feature holds significant promise for the development of antibacterial coatings for medical equipment and implants, as well as for the prevention of bacterial infections. MXene's large surface area and distinct surface chemistry allow it to interact with bacterial cell walls and exert antibacterial properties.<sup>42,43</sup>

MXenes have extraordinary environmental stability and hence can maintain their structural and functional integrity even when subjected to extreme environments.<sup>44</sup> The stability of MXenes is not affected by the presence of acidic, alkaline, or high-temperature conditions. This environmental stability improves the reliability and endurance of biomedical devices and implants based on MXene, which makes it suitable for applications in the field of biomedicine intended to last for an extended period.<sup>3,45</sup>

### 3. Biocompatibility of Ti MXenes vs. non-Ti MXenes

Among the various MXenes, Ti MXenes are mostly explored for biomedical applications. However, the safety issues and the effects of Ti MXenes on human health remain poorly evaluated. As per the study by Wen *et al.*, Ti MXenes cause abnormal neurobehavior and pathological changes as well as accumulation in organs.<sup>46</sup> This is the first report on the effects of Ti MXene nanosheet exposure on pregnancy and offspring. The authors suggested more attention to the long-term effects of MXene exposure, including the health of offspring in adulthood rather than only focusing on the pregnancy outcomes. A recent study by Wei *et al.* showed that  $\text{Ti}_3\text{C}_2\text{T}_x$  nanosheets disrupt spermatogenesis in mice.<sup>47</sup> They observed that high doses of Ti MXene caused oxidative stress in the GC-1 cell line. In another work, Wu *et al.* found dose-dependent cytotoxicity (considerable cell damage and death) on neural stem cells by  $\text{Ti}_3\text{C}_2\text{T}_x$  MXene at a concentration of  $25 \mu\text{g mL}^{-1}$ .<sup>48</sup> However, the effects were less detrimental at lower doses of  $12.5 \mu\text{g mL}^{-1}$ .

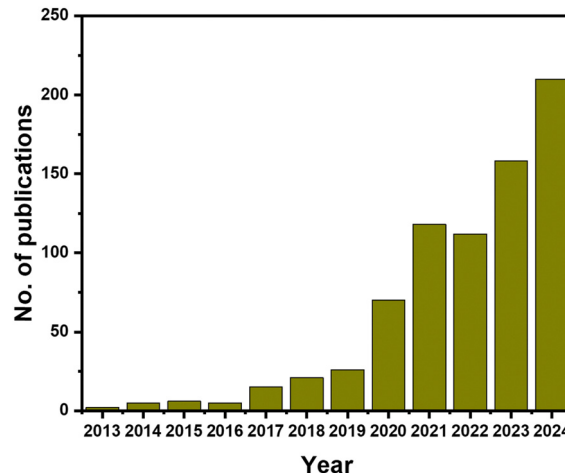


Fig. 2 Trend analysis of annual publications on non-Ti MXenes from 2013 to 2024. Data obtained from Scopus; Copyright © 2024, Elsevier B V.

At  $25 \mu\text{g mL}^{-1}$  dose,  $\text{Ti}_3\text{C}_2$  exposure changed the expression of genes related to stress responses, defense systems, and inflammation, suggesting that cellular stress pathways were activated.

The first non-Ti MXene was discovered by M. Naguib in 2013, and since then, various non-Ti MXenes with central metal atoms, such as Nb, V, and Ta, have been introduced.<sup>49</sup> The bar diagram showing the number of publications on non-Ti MXenes from 2013 to 2024 is shown in Fig. 2. Non-Ti MXenes with central metal atoms, such as Nb, V, and Ta, have been assumed to show much better biocompatibility compared to Ti MXenes.<sup>50</sup> Compared with Ti MXenes, non-Ti MXenes show relatively high stability and resistance to oxidation as well as the possibility of utilizing more environmentally friendly synthesizing procedures for non-Ti MXenes.<sup>51</sup> Non-Ti MXenes, especially Mo-based MXenes, have superior stability compared to Ti-based MXenes<sup>52</sup> and most of the non-Ti MXenes are resistant to oxidation, except V-based MXenes.<sup>53</sup>

Fusco *et al.* investigated the effect of  $\text{Nb}_4\text{C}_3\text{T}_x$  MXenes on the immune system and organs.<sup>54</sup> They observed that  $\text{Nb}_4\text{C}_3\text{T}_x$  neither had any adverse effect on the immune response nor affected gene expression in the cells. It also did not accumulate in the organs of the mice. In another study, Han *et al.* confirmed that the  $\text{Nb}_2\text{CT}_x$  nanosheets functionalized with poly vinyl pyrrolidone (PVP) show promising biocompatibility.<sup>30</sup> The biocompatibility of  $\text{Nb}_2\text{CT}_x$  was further confirmed by Yang *et al.*, who demonstrated promising biocompatibility of  $\text{Nb}_2\text{CT}_x$  quantum dots (QDs) under *in vitro* and *in vivo* conditions and when incubated with myeloperoxidase and  $\text{H}_2\text{O}_2$ .<sup>55</sup> In addition,  $\text{Nb}_2\text{CT}_x$  QDs showed unique biodegradability responsive to human myeloperoxidase. In another recent study, the toxicity of  $\text{Nb}_2\text{CT}_x$  QDs and  $\text{Ti}_3\text{C}_2\text{T}_x$  QDs in human umbilical vein endothelial cells (HUVEC) was compared.<sup>56</sup> It was found that  $\text{Ti}_3\text{C}_2\text{T}_x$  QDs in  $100 \mu\text{g mL}^{-1}$  concentration showed toxicity towards HUVEC when incubated for 24 h, while  $\text{Nb}_2\text{CT}_x$  QDs displayed no toxicity at the same concentration and incubation time. Furthermore,  $\text{Nb}_2\text{CT}_x$  QDs were observed to promote autophagy, while  $\text{Ti}_3\text{C}_2\text{T}_x$  QDs impaired autophagy. It was thus



concluded that compared to  $Ti_3C_2T_x$  QDs,  $Nb_2CT_x$  QDs are more biocompatible to HUVECs under the same experimental conditions.

Feng *et al.* found that  $Mo_2CT_x$  MXene flakes functionalized with poly vinyl alcohol (PVA) display high biocompatibility and biodegradability.<sup>57</sup> The biocompatibility  $V_4C_3T_x$  MXenes were evaluated in several subsets of immune cells, and the MXene showed no cytotoxicity towards the immune cells.<sup>58</sup> The hemolytic activity analysis performed on human red blood cells (RBC) showed that  $V_4C_3T_x$  MXenes did not significantly release hemoglobin (Fig. 3(a)). Additionally,  $V_4C_3T_x$  MXene was not toxic to peripheral blood mononuclear cells (PBMCs) as analysed by cell viability and apoptosis measurement by Annexin V labeling (Fig. 3b). However,  $V_4C_3T_x$  MXene significantly decreased the T cell activation markers CD25 and CD69 (Fig. 3(c)), suggesting potential suppressive effects on the functions of immune cells. Notably,  $V_4C_3T_x$  MXene significantly decreased the secretion of innate inflammatory cytokines in activated PBMC (Fig. 3(d and e)). These results thus show that  $V_4C_3T_x$  MXene exerts immunomodulation by interfering with innate and adaptive immune cell activation. This study not only highlighted the biocompatibility of  $V_4C_3T_x$  MXene but also shed light on the possible application of  $V_4C_3T_x$  MXene in managing inflammatory and autoimmune conditions. All these studies point out that non-Ti MXenes are biodegradable and show better biocompatibility compared to Ti-based MXenes.

Despite the generally acknowledged biocompatibility of vanadium MXene, certain studies present contrasting findings. For example,  $V_2CT_z$  has been observed to undergo *in situ*

oxidation in cell culture media, which can cause cytotoxic effects. The degree of cytotoxicity was observed to be directly proportional to the extent of oxidation, dose, and time. The oxidized vanadium MXene flakes could decrease cell viability through the disintegration of the cellular membrane or by disrupting the cell cycle. This casts a shadow over the biomedical applications of vanadium MXene and its stability.<sup>53</sup>

## 4. Non-Ti MXene-based drug delivery systems for chronic diseases

One reason for the ineffectiveness of cancer treatment is the lack of specificity and side effects of cancer therapies. Most drugs used for cancer treatment have low bioavailability; hence, they are administered in high doses to be effective. However, this causes serious side effects and toxicity.<sup>59</sup> These issues can be addressed using targeted drug delivery systems with specific receptors that can reduce the overall toxicity and increase efficacy.<sup>60</sup> Another major advantage of drug delivery systems is the possibility of efficient combination therapy that increases the potency of the treatment. Along with the combination of different chemotherapeutic drugs, we can enable these systems to aid in photothermal therapy, immunotherapy, and sonodynamic therapy depending upon the material we use to create the drug delivery system. The incorporation of other therapeutic strategies with drug delivery systems further increases the efficacy of the treatment.<sup>61,62</sup> The use of multiple drugs further reduces the toxicity of individual drugs and helps in overcoming drug resistance by cancer cells.

MXenes are excellent candidates for drug delivery systems and combination therapy due to their unique physiochemical features, such as large surface area, mechanical and thermal properties, biocompatibility, and low toxicity.<sup>63</sup> MXene is hydrophilic, which makes it easier to remove from the human biological system. Many researchers have introduced surface moieties, such as folic acid, to make it targeted towards cancer cells because cancer cells have more folate receptors than normal cells. Other than folic acid, many other molecules, such as hyaluronic acid, phospholipids and amino acids, are also being used for surface modification, and these coatings can enhance the biocompatibility of the drug delivery systems.<sup>50</sup>

Non-Ti MXenes, such as Nb, V, Ta and Mo MXenes, have been used in drug delivery systems. These drug delivery systems are either used for drug delivery alone or for synergistic therapy in combination with photothermal therapy, sonodynamic therapy, and nanozyme activity. The next subsection discusses the combinatorial drug delivery approach for various chronic diseases.

### 4.1. Nb MXenes as combinatorial therapeutic systems

Nb-based MXenes have been explored in drug delivery applications mainly in combination therapy and theranostics. One such synergistic approach was developed by Hao *et al.* in which  $Nb_2CT_x$  MXene-based plasmonic assembly loaded with Pt nanozymes, and doxorubicin (DOX) was used for combined

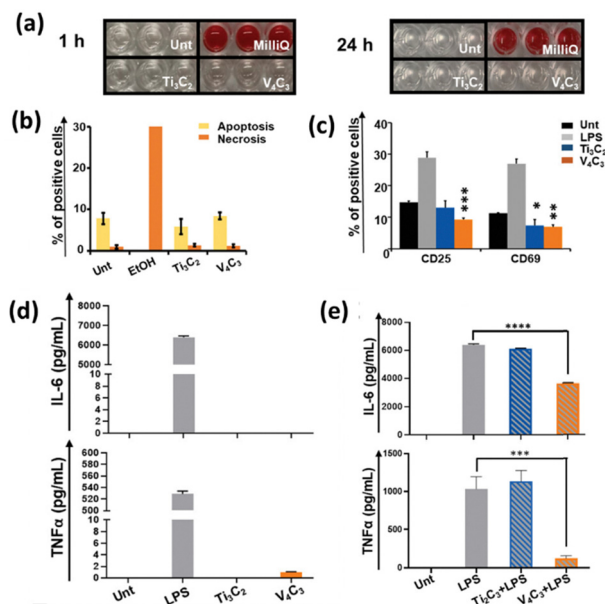


Fig. 3 (a) Hemolysis assay performed on human red blood cells (RBCs). The red color solution is due to the release of hemoglobin from lysed RBCs. (b) PBMCs treated with  $50 \mu\text{g mL}^{-1}$  of  $V_4C_3T_x$  or  $Ti_3C_2T_x$  for 24 h, stained with Annexin V and Fixable Viability Staining 780 and analyzed by flow cytometry. (c) Immune cell activation marker staining analysis by flow cytometry. (d) and (e) Evaluation of cytokine (IL-6, and TNF $\alpha$ ) concentrations in supernatants of PBMCs. Reprinted with permission from ref. 58 Copyright © 2024, Wiley-VCH GmbH.



drug delivery, nanozymes, and photothermal therapy.<sup>64</sup> The assembly contained a tumor cytomembrane used for tumor targeting. In cancer cells, the hypoxic condition and low pH trigger the release of DOX, and the Pt nanozyme is activated when irradiated with an NIR-II laser. The Pt nanozymes can trigger the production of reactive oxygen species, leading to the death of cancer cells.

In another work, Nb<sub>2</sub>CT<sub>x</sub> combined with mesoporous silica was used as a perfect platform for drug delivery along with photothermal therapy.<sup>65</sup> Here, cetanecyltrimethylammonium chloride (CTAC) was used as the surfactant for mesopore formation, and the composite was modified with polyethylene glycol (PEG), followed by arginine-glycine-aspartic pentapeptide (RGD) conjugation. The synthesized composite acts as a drug and targets cancer cells through the selective binding of integrin overexpressed on the cancer cell membrane. The composite exhibited high photothermal conversion capability in the presence of laser irradiation in the NIR-II region (1064 nm), which resulted in the maximum elimination of cancer cells (U-87). Similarly, an immune adjuvant drug R837 (Imiquimod, an agonist of toll-like receptor 7) was loaded on polydopamine (PDA) modified Nb<sub>2</sub>CT<sub>x</sub> for cancer photothermal/immune-therapy in the NIR-II biowindow.<sup>66</sup> The PDA functionalization of Nb<sub>2</sub>CT<sub>x</sub> enhances the loading rate and stability of the system. An RBC membrane was applied as a coating in this system to prevent the clearance of the nanocomposite system by phagocytosis. Due to the toll-like receptor 7-signaling, R837 modification enhances the maturation and activation of dendritic cells (DCs) and hence superior immune responses that inhibit secondary tumors as well as tumor recurrence compared to photothermal therapy without R837.

Apart from photothermal therapy in combination with drug delivery, Nb MXene can be utilized for sonodynamic therapy along with drug delivery. In sonodynamic therapy, low-intensity ultrasound and sonosensitizers are combined to produce ROS that can be utilized to destroy bacteria or tumors. Sonodynamic therapy has fewer side effects and achieves deep tissue penetration in biological tissue up to 40 mm thickness, which is approximately five times more than the tissue penetration by NIR.<sup>67</sup> Pang *et al.* used poly(vinylpyrrolidone) (PVP) functionalized Nb<sub>2</sub>CT<sub>x</sub> nanosheets for loading the polythiophene-based sonosensitizer towards sonodynamic therapy for solid tumors.<sup>68</sup> Utilizing the catalase-like activity of Nb<sub>2</sub>CT<sub>x</sub> could catalyze the conversion of H<sub>2</sub>O<sub>2</sub> to O<sub>2</sub>, and this lessens the tumor hypoxia and cell activity and enhances the efficacy of sonodynamic therapy. Upon ultrasound irradiation, the nanosheets release the sonosensitizer and produce both singlet oxygen and superoxide anions. This process led to tumor cell death with enhanced sonodynamic therapy efficacy.

It was found that Nb MXenes can also induce programmed cell death (or apoptosis) in cancer cells. Jastrzebska *et al.* modified Nb<sub>4</sub>C<sub>3</sub>T<sub>x</sub> and Nb<sub>2</sub>CT<sub>x</sub> with polylysine to convert the surface charge of MXene to positive and evaluated cell cycle arrest and apoptosis in melanoma cells.<sup>69</sup> They also found that polylysine-modified Nb MXene had ROS scavenging activities, showing the pivotal role played by surface modifications of

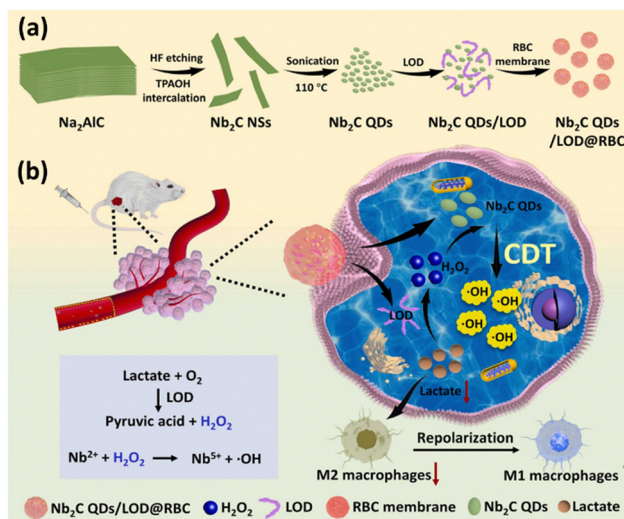


Fig. 4 Schematics of the (a) synthesis of Nb<sub>2</sub>CT<sub>x</sub> QDs/LOD@RBC and (b) its catalytic activity in lactate consumption and macrophage repolarization for enhanced chemodynamic therapy. Reprinted with permission from Ref. 70 Copyright © 2022, Elsevier B.V.

MXene in determining the functions and characters in cell cycle arrest and inducing apoptosis.

Chemodynamic therapy utilizes the ability of chemodynamic materials to selectively induce tumor cell apoptosis *via* Fenton or Fenton-like reactions, and it is considered highly effective in tumor-specific treatments. Nb<sub>2</sub>CT<sub>x</sub> QDs have been used for chemodynamic therapy by modifying it with lactate oxidase (LOD) and RBC encapsulation.<sup>70</sup> The schematics of the synthesis of Nb<sub>2</sub>CT<sub>x</sub> QDs/LOD@RBC and its catalytic activity in lactate consumption and macrophage repolarization for enhanced chemodynamic therapy are depicted in Fig. 4. The nanocomposite could convert H<sub>2</sub>O<sub>2</sub> into <sup>•</sup>OH, while the overexpressed lactate could be catalyzed into H<sub>2</sub>O<sub>2</sub> by lactate oxidase to replenish the depletion of H<sub>2</sub>O<sub>2</sub>. This, in turn, disrupts the tumour microenvironment, making it more accessible to immunostimulatory macrophages. This might result in maximizing the therapeutic outcome of the chemodynamic therapy.

In addition to standard anticancer drugs, Nb<sub>2</sub>CT<sub>x</sub> nanosheets can also be used to carry natural molecules. Ultrathin Nb<sub>2</sub>CT<sub>x</sub> nanosheets functionalized with berberine, a natural inhibitor of cancer metastatic proteins was used for synergistic therapy for breast cancer and subsequent lung metastasis.<sup>71</sup> The nanocomposite exhibited promising biocompatibility and drug loading while maintaining photothermal performance and anticancer efficacy. It was concluded that the functionalized Nb<sub>2</sub>CT<sub>x</sub> nanoplatform efficiently destroys cancer cells and inhibits metastasis with minimal local tissue damage.

In addition to cancer treatments, researchers are exploring the application of Nb<sub>2</sub>CT<sub>x</sub> in treating various other diseases, such as neurodegenerative conditions and infections. Du *et al.* successfully used an ultrathin Nb<sub>2</sub>CT<sub>x</sub> nanosheet as an interesting metal-ion chelating agent and an artificial nanozyme for catalysing ROS scavenging.<sup>72</sup> The Nb<sub>2</sub>CT<sub>x</sub> nanosheets capture



$\text{Cu}^{2+}$  so that the coordination between  $\text{Cu}^{2+}$  and  $\text{A}\beta$  aggregate suppresses and protects tissues from  $\text{Cu}^{2+}$ -associated toxicity. In addition, the nanosheets exhibit an enhanced permeability to the blood brain barrier and excellent photothermal effect under the NIR-II laser irradiation.

#### 4.2. V MXenes as combinatorial therapeutic systems

$\text{V}_2\text{CT}_x$  MXene has been used in biomedicine due to its excellent photothermal conversion, drug loading properties, biocompatibility, and biodegradable characteristics.  $\text{V}_2\text{CT}_x$  MXene loaded with DOX was explored for the delivery of DOX and for the evaluation of the growth inhibition and metastasis of triple-negative breast cancer.<sup>73</sup> This work is based on the local “heat” generation that could occur at tumor sites in the presence of an NIR laser and the controlled release of DOX that results in the potent inhibition of tumor growth and metastasis. They also proposed that hyperthermia in conjunction with the acidic and  $\text{H}_2\text{O}_2$ -rich tumor microenvironment would accelerate the decomposition of  $\text{V}_2\text{CT}_x$ , leading to controlled DOX release.

$\text{V}_4\text{C}_3\text{T}_x$  MXene nanozyme causes redox imbalance in the tumor microenvironment that disrupts cancer mass and elimination of cancer cells. For the nanozyme catalytic/photothermal therapy of cancer, Zhao *et al.* functionalized MXene with Atovaquone (ATO), a commonly used antimalarial drug and natural inhibitor of electron transport chain.<sup>74</sup> The antitumor mechanism of  $\text{V}_4\text{C}_3\text{T}_x$  MXene by interfering with tumor redox homeostasis in the ATO-enhanced nanozyme catalytic/photothermal therapy is illustrated in Fig. 5. The authors designed a system with  $\text{V}_4\text{C}_3\text{T}_x$  and ATO encapsulated with bovine albumin (BSA). The stable and strong photothermal effect of the nanocomposite under NIR irradiation causes the necrosis of tumor cells with enhanced peroxidase-like activity. The released ATO suppresses the cellular respiration in the mitochondria, leading to decreased ATP levels and expression of heat shock proteins. In addition, the nanocomposite exhibits high photoacoustic and photothermal imaging performances.<sup>74</sup>

It has been observed that chronic inflammation can be a potential precursor to cancer. This can be observed in conditions such as colitis, wherein acute or chronic inflammation of

the mucosal lining of the colon may lead to colorectal cancer. Hence, proper management of inflammation is critical. Recently,  $\text{V}_2\text{CT}_x$  with gallium doping was reported to alleviate inflammation in the colon mucosal lining by reducing the excessive reactive oxygen species and proinflammatory cytokines.<sup>75</sup> This is attributed to numerous enzyme mimicking activities of  $\text{V}_2\text{CT}_x$  MXene. Additionally, the controlled release of gallium under NIR irradiation helps in complete tumor ablation without further recurrence.

Photothermal therapy based on MXenes is gaining momentum, but the major issue with this therapy is that cancer cells are slowly acquiring resistance. Heat shock proteins provide thermo-resistance to cancer cells. This heat resistance issue was addressed by a research group using  $\text{V}_2\text{CT}_x$  QDs with a low-temperature nucleus-targeted photothermal therapy strategy in the NIR-II region.<sup>76</sup> Here, the  $\text{V}_2\text{CT}_x$  QDs were functionalized with TAT peptides and engineered exosome vectors. These modifications provided good biocompatibility, long circulation time, and endosomal escape ability to the nanoparticles, and they could enter the nucleus of the target cell for low-temperature photothermal therapy with enhanced tumor destruction efficiency.

#### 4.3. Ta MXenes as combinatorial therapeutic systems

Investigations of the biomedical applications of Ta MXenes are very limited. Rafieerad *et al.* used  $\text{Ta}_4\text{C}_3\text{T}_x$  MXene QDs for the *in vivo* treatment of transplant vasculopathy.<sup>77</sup> They confirmed the biocompatibility of  $\text{Ta}_4\text{C}_3\text{T}_x$  QDs on human cells, which mainly originated from the tantalum oxides ( $\text{TaO}_2$  and  $\text{Ta}_2\text{O}_5$ ) present on the MXene surface. These  $\text{Ta}_4\text{C}_3\text{T}_x$  QDs were internalized in endothelial cells and reduced the endothelial cell-mediated activation of  $\text{IFN-}\gamma$  + Th1 cells. From a quantitative polymerase chain reaction (qPCR)-based gene expression analysis of common immunologic pathways, they found that  $\text{Ta}_4\text{C}_3\text{T}_x$  QDs cause a significant shift in the expression patterns of PDL-1 and CD-86. PD-L1 is a co-inhibitory molecule, while CD-86 is a co-stimulatory molecule for T-cell activation. This dual action inhibits pro-inflammatory Th1 responses and diminishes immune cell infiltration, including cytotoxic CD8+ T-cells, while enhancing regulatory T-cells (Tregs), which are crucial for immunological tolerance. Further, in an *in vivo* model of organ transplant rejection,  $\text{Ta}_4\text{C}_3\text{T}_x$  QDs reduced the immune cell infiltration and structural degeneration within transplanted tissues. Overall,  $\text{Ta}_4\text{C}_3\text{T}_x$  QDs can be used for immunoengineering and other biomedical applications.

#### 4.4. Mo MXenes as combinatorial therapeutic systems

Molybdenum-based MXenes have received relatively limited exploration in the domain of biomedical applications.<sup>52</sup> Similar to other MXenes, Mo-based MXenes are also explored for photothermal therapy applications. Feng *et al.* used  $\text{Mo}_2\text{CT}_x$  MXene flakes functionalized with PVA with high biocompatibility and biodegradability for photothermal activity against 4T1 breast cancer cells.<sup>57</sup> They found that the  $\text{Mo}_2\text{CT}_x$ -PVA nanoflakes alone show relatively low toxicity to cancer cells. However, upon irradiation,  $\text{Mo}_2\text{CT}_x$ -PVA nanoflakes increase

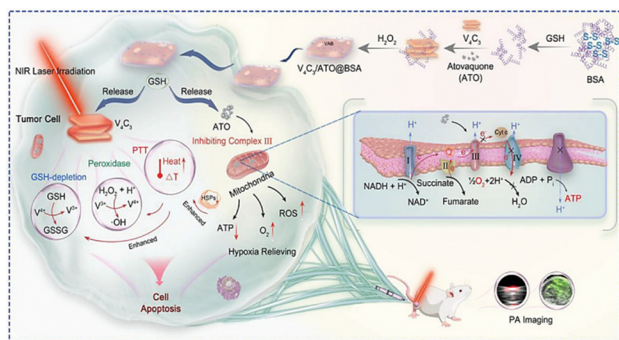


Fig. 5 Schematic of the antitumor mechanism of  $\text{V}_4\text{C}_3\text{T}_x$  MXene in ATO-enhanced nanozyme catalytic/photothermal therapy by tumor redox homeostasis. Reprinted with permission from ref. 74 Copyright © 2023, Wiley-VCH GmbH.



Table 1 Summary of non-Ti MXenes based combinational treatments tested for various diseases

Nano system	Therapeutic strategies	Mode of action	Model used	Ref.
Nb <sub>2</sub> CT <sub>x</sub> -Pt-DOx@M	Drug delivery, photothermal therapy, nanozymes	Delivery of DOX is enhanced by NIR irradiation. Photothermal therapy creates ROS and further increases treatment efficiency. Pt nanozymes generate oxygen and disturb the hypoxic environment	<i>In vitro</i> -HeLa cell line <i>In vivo</i> -Kunming mice model	64
CTAC@Nb <sub>2</sub> CT <sub>x</sub> -MSN-PEG-RGD	Chemotherapy and photothermal therapy	RGD-tagged system efficiently accumulates in tumor sites and photothermal therapy supported by chemotherapy efficiently destroys the cancer cells	<i>In vitro</i> -U87 cell line <i>In vivo</i> -nude mice model	65
Nb <sub>2</sub> CT <sub>x</sub> @PDA-837@RBC	Immunotherapy and photothermal therapy	Photothermal therapy destroys the cancer cells and the immunoadjuvants attached to it trigger immunotherapy	<i>In vitro</i> -4T1 cell line <i>In vivo</i> -BALB/c mice	66
Nb <sub>2</sub> CT <sub>x</sub> -Berberine	Chemotherapy and photothermal therapy	Photothermal therapy generates ROS and triggers the release of drugs, which leads to cell death	<i>In vitro</i> -4T1, MDA-MB-231, RAW 264.7 cell line <i>In vivo</i> -mice	71
Nb <sub>2</sub> CT <sub>x</sub>	Nanozyme effect and photothermal therapy	ROS scavenging, Removal of Cu <sup>2+</sup> ions	<i>In vitro</i> -SH-SY5Y cell line <i>In vivo</i> -ICR mice	72
Nb <sub>2</sub> CT <sub>x</sub> -PVP-PT2	Sonodynamic therapy and nanozyme effect	Catalase-like activity Nb <sub>2</sub> C MXene disrupts the hypoxic condition of the tumor, and this increases the efficacy of sonodynamic therapy	<i>In vitro</i> -4T1 cell line <i>In vivo</i> -BALB/c mice	68
Nb <sub>2</sub> CT <sub>x</sub> QD/LOD@RBC	Immunotherapy and chemodynamic therapy	Lactate oxidase consumes H <sub>2</sub> O <sub>2</sub> in the tumor microenvironment and triggers M1-Macrophage infiltration and the CDT agent triggers apoptosis of the cancer cells	<i>In vitro</i> -4T1, RAW264.7 cell line <i>In vivo</i> -BALB/c mice	70
V <sub>2</sub> CT <sub>x</sub> -DOX@Gel	Chemotherapy and photothermal therapy	NIR 808 nm irradiation triggers the release of DOX	<i>In vitro</i> -MCF-7, MDA-MB-231, MCF-10A cell line <i>In vivo</i> -BALB/c nude mice	73
V <sub>4</sub> C <sub>3</sub> T <sub>x</sub> /ATO@BSA	Nanozyme and photothermal therapy	Nanozyme activity disrupts the tumor microenvironment and photothermal therapy destroys the cancer cells	<i>In vitro</i> -L929, 4T1, cell line <i>In vivo</i> -BALB/c mice	74
Ga-V <sub>2</sub> CT <sub>x</sub> -NH <sub>2</sub>	Nanozyme and photothermal therapy	Nanozyme activity alleviates inflammation, and the photothermal effect leads to cancer cell death	<i>In vitro</i> -HUVEC, NCM460 cell line <i>In vivo</i> -BALB/c nude mice	75
V <sub>2</sub> CT <sub>x</sub> QDs	Photothermal therapy with nuclease targeting	Nuclease targeting and subsequent photothermal effect	<i>In vitro</i> -MCF-7, A549, NHDF cell line <i>In vivo</i> -BALB/c nude mice	76
Ta <sub>4</sub> C <sub>3</sub> T <sub>x</sub> QDs	Drug delivery with immunotherapy	Anti-inflammatory and antiapoptotic properties, Intrinsic immunomodulation for the treatment of allograft vasculopathy	<i>In vitro</i> -HUVEC, PBMNC cell line <i>In vivo</i> -Lewis rat, Sprague-Dawley rat	77
Mo <sub>2</sub> CT <sub>x</sub> -PVA	Photothermal therapy	Photothermal activity against 4T1 breast cancer cells. Highly biodegradable	<i>In vitro</i> -4T1, L929 cell line <i>In vivo</i> -BALB/c nude mice	57
Mo <sub>2</sub> CT <sub>x</sub> @MoO <sub>x</sub>	Photothermal heating along with chemodynamic therapy	ROS production for inducing cancer cell death	<i>In vitro</i> -HeLa cell line <i>In vivo</i> -BALB/c nude mice	78

the permeability of the lysosomal membrane, leading to its collapse, mitochondrial fragmentation, and actin filament defects. These disruptions ultimately lead to cancer cell death.

Along with photothermal therapy, Wang *et al.* used Mo<sub>2</sub>CT<sub>x</sub>@MoO<sub>x</sub> nanoclusters to produce ROS to induce cancer cell death.<sup>78</sup> They found that the carbon-supported Mo<sub>2</sub>CT<sub>x</sub>@MoO<sub>x</sub> efficiently catalyzed the formation of ROS from the endogenous H<sub>2</sub>O<sub>2</sub>, and the presence of high dispersion of active Mo<sup>5+</sup> sites could enhance the ROS efficiency of Mo<sub>2</sub>CT<sub>x</sub>@MoO<sub>x</sub>. In addition, the Mo<sub>2</sub>CT<sub>x</sub> core in the Mo<sub>2</sub>CT<sub>x</sub>@MoO<sub>x</sub> nanoclusters promotes photothermal heating, along with chemodynamic therapy by Mo<sup>5+</sup>/Mo<sup>6+</sup> species that could be continued by glutathione (GSH) consumption. In short, the Mo<sub>2</sub>CT<sub>x</sub>@MoO<sub>x</sub> nanoclusters can be used for cancer therapy through the production of ROS and NIR-II photothermal

activity. Table 1 summarizes the use of non-Ti MXenes for combinational treatments tested for various diseases.

## 5. Non-Ti MXenes as nanozymes

Nanozymes are nanoparticles that exhibit enzyme-like activities and carry out the catalytic process of naturally occurring enzymes.<sup>79</sup> The enzyme mimetic abilities of nanozymes can be modulated by factors such as pH, H<sub>2</sub>O<sub>2</sub>, the chemical nature of metal ions, and glutathione levels. These nanozymes have gained great attention in the biomedical field due to their high stability and cost-effectiveness and have been used as an alternative for naturally occurring enzymes. MXenes can exhibit enzyme-like activities, and the MXenes showing nanozyme



activity are termed MXenzymes. This nanozyme ability of MXene can be utilized for both sensing and therapeutic purposes. MXenes have been reported to exhibit catalytic activities that mimic superoxide dismutase, catalase, peroxidase, and others. MXenes have an intrinsic peroxidase-like activity that may interfere with the efficiency and stability of the nanozyme. The exact mechanism by which MXene exhibits these features has not yet been identified. Even though MXenes are used as nanozymes in the biomedical field, the stability of MXene is one of the limitations that can restrict MXene for use as MXenzymes. The stability issue can be addressed by engineering composites of MXenes; however, the composites can also influence the enzyme-mimicking activity of the MXene. It has been established that non-Ti MXenes, such as Nb, V and Ta MXenes, have excellent nanozyme activities.<sup>50,80–82</sup>

## 6. Theranostic applications of non-Ti MXenes

Theranostics is the procedure in which diagnosis and treatment are carried out by the same system, and it has an incredible future in oncology, especially due to the rise of nanoparticles. MXenes are excellent candidates for theranostics because they can be used for drug delivery, immunotherapy, sonodynamic therapy, and photothermal therapy for treating cancer, and the same system can be utilized for imaging the cancer and sensing the biomarkers.<sup>83</sup> Lin *et al.* utilized the Nb<sub>2</sub>CT<sub>x</sub> nanosheets functionalized with PVP for photothermal thermal therapy against breast cancer and for the photoacoustic imaging of tumors.<sup>30</sup> It was found that the Nb<sub>2</sub>CT<sub>x</sub>-PVP nanosystem possesses low phototoxicity, great biocompatibility, and unique enzyme-responsive biodegradability to myeloperoxidase. The developed nanosystem showed highly efficient *in vivo* photothermal tumor eradication properties in both NIR-I and NIR-II biowindows. Moreover, *in vivo* photoacoustic imaging was performed on 4T1-tumor-bearing mice after intravenous administration, and the results demonstrated the potential of Nb<sub>2</sub>CT<sub>x</sub>-PVP nanosheets for photoacoustic imaging.

As a tumor microenvironment stimuli-responsive theranostic nanoplatfoms, Nb<sub>2</sub>CT<sub>x</sub> functionalized with Fe<sub>3</sub>O<sub>4</sub> and MnO<sub>x</sub> was used for dual-modality magnetic resonance (MR) imaging-guided photothermal ablation of breast cancer.<sup>84</sup> The developed nanoplatfom showed high photothermal-conversion efficiency in the NIR-II biowindow with highly efficient photothermal tumor eradication without reoccurrence. It has also shown enhanced biocompatibility and tumor microenvironment responsive T1- and T2-weighted MR imaging capability. With the addition of MnO<sub>x</sub>, mild acidic conditions and an elevated reducing microenvironment could result in tumor microenvironment sensitive T1-weighted MR imaging. Until MnO<sub>x</sub> disintegrates, the incorporated superparamagnetic Fe<sub>3</sub>O<sub>4</sub> could serve as a T2-weighted MR imaging contrast agent. This tumor microenvironment responsive T1- and T2-weighted MR imaging with such high efficiency enhances treatment guidance and monitoring.

In another work, Cao *et al.* used V<sub>2</sub>CT<sub>x</sub> QDs coated with exosome and RGD peptide for low-temperature nucleus-targeted photothermal therapy. These nanoparticles also exhibited the potential of fluorescent imaging, photoacoustic imaging (PAI), and MR imaging.<sup>76</sup> The fluorescent V<sub>2</sub>CT<sub>x</sub> QDs showed good photothermal effects in the NIR-II region, and the modification with TAT peptides and packaged into an engineered exosome with RGD modification provided good biocompatibility, long circulation time, and endosomal escape ability. Hence, these nanoparticles can easily target the cell and enter the nucleus for low-temperature nucleus-targeted photothermal therapy.

Ta<sub>4</sub>C<sub>3</sub>T<sub>x</sub> MXenes have also been used for theranostic applications mainly for imaging-guided photothermal tumor ablation. Dai *et al.* used a composite material made of Ta<sub>4</sub>C<sub>3</sub>T<sub>x</sub> MXene with MnO<sub>x</sub> for multiple imaging-guided photothermal tumor ablation.<sup>85</sup> The developed nanocomposite showed its adaptability by acting as a contrast agent for photoacoustic imaging, tumor microenvironment-responsive T1-weighted MR imaging, and computed tomography (CT). A thorough and complete image of the tumor and its microenvironment was possible with this multi-modal imaging technique.<sup>85</sup> Here, the tantalum component in the composite acts as the contrast agent for contrast-enhanced computed tomography, while the MnO<sub>x</sub> component acts as the tumor microenvironment-responsive contrast agent for T1-weighted MR imaging. Thus, in addition to contrast-enhanced photoacoustic imaging, the photothermal-conversion performance of the MnO<sub>x</sub>/Ta<sub>4</sub>C<sub>3</sub>T<sub>x</sub> composite imparts significant tumor growth suppression by photothermal hyperthermia.

In another study, Lin *et al.* explored ultrathin biocompatible Ta<sub>4</sub>C<sub>3</sub>T<sub>x</sub> nanosheets modified with soybean phospholipid (SP) for photoacoustic (PA)/computed tomography (CT) imaging and photothermal ablation of tumors *in vivo*.<sup>86</sup> The schematic presentations on the synthesis of Ta<sub>4</sub>C<sub>3</sub>T<sub>x</sub> nanosheets, surface modification with SP, and *in vivo* dual-mode imaging combined with photothermal therapy are depicted in Fig. 6. The outstanding photothermal capacity of the Ta<sub>4</sub>C<sub>3</sub>T<sub>x</sub> nanosheets with photothermal conversion efficiency resulted in the effective elimination of cancer cells. Besides, the high NIR absorption and strong X-ray attenuation make them efficient contrast agents for imaging applications.

## 7. Antibacterial activity of non-Ti MXenes

Generally, the antibacterial properties of 2D materials have been associated with the production of ROS, and penetration of the bacterial cell membrane, causing bacterial cell death.<sup>87</sup> In particular, the antimicrobial properties of 2D materials, such as graphene, are observed from oxidative and physical stresses triggered by the sharp edges of graphene nanosheets, potentially causing damage to bacterial cell membranes and compromising their integrity.<sup>43</sup> Consequently, MXene-based materials, akin to graphene-like nanomaterials, show similar activity and hold immense promise in antibacterial applications. Rasool *et al.*



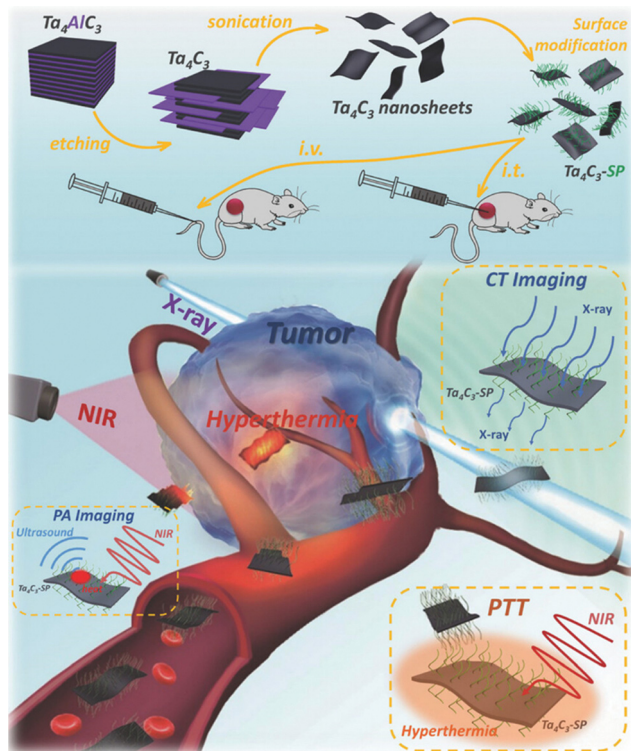


Fig. 6 Schematics of the synthesis of  $Ta_4C_3T_x$  nanosheets, surface modification with SP, and *in vivo* PA/CT dual-mode imaging combined with photothermal therapy. Reprinted with permission from ref. 86 Copyright © 2018, Wiley-VCH GmbH.

investigated the antibacterial activity of MXene for the first time and found that  $Ti_3C_2T_x$  nanosheets can stimulate antibacterial activity in a dose-dependent manner and that the activity was superior in comparison with graphene oxide.<sup>43</sup> They also proposed that the direct contact of bacteria with  $Ti_3C_2T_x$  MXene can disrupt cellular membranes, leading to cell damage and eventual death.

The antibacterial activities of  $Nb_2CT_x$  and  $Nb_4C_3T_x$  nanosheets were evaluated by Pandey *et al.* using model Gram-negative and Gram-positive bacteria.<sup>88</sup> They found that the bactericidal properties of  $Nb_2CT_x$  and  $Nb_4C_3T_x$  depend on the sheet size and atomic structure of both MXenes (Fig. 7). Furthermore, the antibacterial activity increased with a decrease in the lateral sheet size.  $Nb_4C_3T_x$  nanosheets possess higher antibacterial activity than  $Nb_2CT_x$  owing to the higher oxidative stress. In another work, Wojciechowska *et al.* found that surface-functionalization of Nb MXene with lysozyme enhances the antibacterial activity owing to a change in the surface charge from negative to positive.<sup>89</sup> In contrast, the collagen functionalized  $Nb_4C_3T_x$  exhibited the growth enhancement of *Bacillus subtilis* by 225%, thus showing the bio-tunability of MXene.

Recently, amidated titanium plates (TP) were utilized as a platform for the preparation of a biofunctional therapeutic system termed  $Nb_2CT_x@TP$  by grafting  $Nb_2C$  nanosheets onto them for bacterial clearance and tissue regeneration.<sup>90</sup> Although increasing  $Nb_2CT_x$  concentrations led to only a

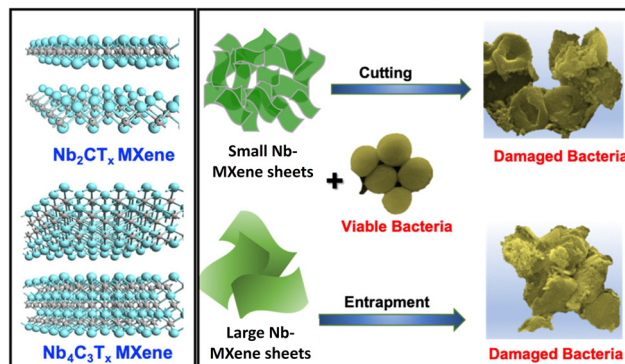


Fig. 7 Size-dependent antibacterial strategy of Nb-MXenes. Reprinted with permission from ref. 88. Copyright © 2020 the American Chemical Society.

slight bacterial death, there was a remarkable reduction in live bacteria biofilm. Notably, on the surface of  $Nb_2CT_x@TP$ , bacteria exhibited rupture, indicating their efficacy in inhibiting biofilm formation and inducing bacterial death. Upon exposure to an 808 nm laser, bacterial colonies and survival rates of *S. aureus* and *E. coli* were progressively decreased in the  $Nb_2CT_x@TP$  groups by increasing irradiation time. Transmission electron microscopy (TEM) imaging depicted blurry cell walls and membranes of *S. aureus* and *E. coli* bacteria, disrupted cellular bubbles, and distorted cytoplasmic structures. Hyperthermia induced by  $Nb_2CT_x@TP$  caused the detachment of cilia and flagella, thus inhibiting bacterial spread and biofilm formation. Lactate dehydrogenase (LDH) tests and *ortho*-nitrophenyl- $\beta$ -galactoside (ONPG) hydrolysis tests confirmed that thermotherapy with  $Nb_2CT_x@TP$  could disrupt bacterial membranes and induce bacterial death. Furthermore, laser-activated  $Nb_2CT_x@TP$  mitigated excess ROS production, which reduced the proinflammatory reaction and upregulated vascular endothelial growth factors, thereby promoting angiogenesis, tissue regeneration, and wound healing. In another work, Yang *et al.* reported the integration of a porphyrin metal-organic framework (MOF) with  $Nb_2CT_x$  as a sonosensitizer for antibacterial therapy and bone regeneration.<sup>91</sup> In this study, the ultrasonic currents from the developed sonosensitizer successfully prompted stem cell differentiation by facilitating the cation transport and ATP-synthesis-linked electron transport. This study provides a new strategy to eliminate infections and to treat osteomyelitis by promoting bone regeneration.

The antibacterial activity of  $Nb_2CT_x$  has been used in wound healing applications. In this aspect, Yang *et al.* developed an antibacterial  $Nb_2CT_x$  MXene hydrogel with enhanced oxidative stress aiming at eradicating the methicillin-resistant *Staphylococcus aureus* (MRSA) bacterial infection and accelerating MRSA-infected wound healing.<sup>92</sup> Similarly, Chen *et al.* developed an anti-oxidative and thermosensitive  $Nb_2CT_x$  MXene-based hydrogel with improved antimicrobial activity for promoting diabetic wound healing.<sup>93</sup> The results confirmed that the  $Nb_2CT_x$  hydrogel stimulates wound healing by reducing oxidative damage, attenuating ROS levels, accelerating angiogenesis and eliminating bacterial infection under NIR irradiation.



In another work, Yuan *et al.* used CeO<sub>2</sub>-Nb<sub>2</sub>CT<sub>x</sub> nanocomposite with both nanozyme and photothermal activity to kill bacteria in a diabetic wound.<sup>94</sup> The nanocomposite obtained maximum elimination of bacteria by both catalytic activity and photothermal effect under NIR irradiation at 808 nm. They found that the composite can accelerate wound healing in rat models and thus provides a new antibacterial strategy by combining catalytic sterilization with the NIR photothermal activity for the effective treatment of diabetic wound infection.

Other than Nb MXenes, both Mo and V MXenes have also been evaluated for their antibacterial activity. In a recent study by Chen *et al.*, oxygen-vacancy-rich MoO<sub>x</sub> directly on fluorine-free Mo<sub>2</sub>CT<sub>x</sub> was synthesized with unique neural network-like structures.<sup>95</sup> These nanonetworks demonstrated excellent antibacterial efficacy, driven by their ability to capture bacteria and generate robust ROS when subjected to precise ultrasound (US) irradiation. The exceptional broad-spectrum microbicidal activity of MoO<sub>x</sub>@Mo<sub>2</sub>CT<sub>x</sub> nanonetworks, without causing harm to normal tissues, was substantiated through comprehensive *in vitro* and *in vivo* assessments. In another work, Lv *et al.* introduced boron dipyrromethene (BODIPY)-modified Mo<sub>2</sub>CT<sub>x</sub> nanosheets (BODIPY-Mo<sub>2</sub>CT<sub>x</sub>) with appropriate antibacterial properties using both photothermal and photodynamic effects.<sup>96</sup>

The antibacterial property of V<sub>2</sub>CT<sub>x</sub> nanosheets was evaluated by Zada *et al.* as a promising photothermal agent for bacterial elimination.<sup>97</sup> The results showed that about 99.5% of both Gram-positive *S. aureus* and Gram-negative *E. coli* could be killed with a low dose of V<sub>2</sub>CT<sub>x</sub> NSs suspension (40 μg mL<sup>-1</sup>) with 5 min NIR irradiation. Similarly, Zhang *et al.* evaluated the antibacterial activity of V<sub>2</sub>CT<sub>x</sub> nanosheets in the presence of NIR irradiation.<sup>98</sup> They found that only 20 μg mL<sup>-1</sup> V<sub>2</sub>CT<sub>x</sub> was able to achieve efficient photothermal sterilization that can be used for the clinical treatment of diseases caused by multidrug-resistant bacteria. In another work, a composite of four-armed host-defense peptidomimetic 4 K10 and V<sub>2</sub>CT<sub>x</sub> was synthesized and evaluated owing to its antibacterial activity.<sup>99</sup> The synthesized 4 K10@V<sub>2</sub>CT<sub>x</sub> nanosheets exhibited promising *in vitro* antimicrobial activity against MRSA and *Pseudomonas aeruginosa* at a low photothermal temperature of 54.1 °C. Based on the data from human *ex vivo* skin infection models, 4 K10@V<sub>2</sub>CT<sub>x</sub> could be used to eradicate the biofilm-associated infections of the skin caused by MRSA bacteria.

Lian *et al.* found that the V<sub>2</sub>CT<sub>x</sub> nanosheets have distinctive oxidase-like activity and exhibit excellent broad-spectrum antibacterial activity due to the production of ROS.<sup>100</sup> In another work, He *et al.* introduced Pt@V<sub>2</sub>CT<sub>x</sub> composite with NIR-II and chemodynamic therapy enhanced dual enzyme-like activity.<sup>101</sup> They found that Pt@V<sub>2</sub>CT<sub>x</sub> eliminates MRSA strain from deep-seated tissues in subcutaneous abscesses and bacterial keratitis environments, promoting wound and cornea healing.

Other than V<sub>2</sub>CT<sub>x</sub> MXene, V<sub>2</sub>NT<sub>x</sub> MXene has also been used to produce ROS to destroy germs and to promote the healing of subcutaneous abscesses with minimum toxicity.<sup>102</sup> The authors have also found that it can function as a nanozyme for photothermal-enhanced anti-infective therapy and the catalytic activity of nanozyme was significantly enhanced through the

photothermal effect. This can produce a large quantity of ROS without local hyperthermia, which otherwise can damage the normal skin tissue. Consequently, V<sub>2</sub>NT<sub>x</sub> may represent a promising candidate for effective anti-infective therapy.

The exploration of double-transition MXenes is in the infant stage, and very few studies have been conducted on this exploration. The double transition-metal TiVCT<sub>x</sub> MXene displayed antibacterial properties (up to 99%) against *Escherichia coli*.<sup>103</sup> Similar antibacterial properties (up to 100%) were also achieved with Ti<sub>3</sub>C<sub>2</sub>T<sub>x</sub> MXene. The authors suggested that the antibacterial mechanism is due to the presence of sharp edges that act as “nano-knives” and cause physical damage to bacterial cell membranes by direct physical interaction. The TiVCT<sub>x</sub> MXene also shows efficient photothermal conversion that decreases the temperature required to kill bacteria without causing any damage to normal tissue. Table 2 shows a comparison of the antibacterial activity of the non-Ti MXenes reported recently.

The proposed bacterial inhibition mechanisms of MXenes include mainly three modes of action namely, nano-knife, ROS generation and nanothermal blades (Fig. 8), which are briefly discussed in the subsequent sections.

### 7.1. Nano-knife mechanism

The inherent negative charge in MXene affects its interaction with bacteria to some extent, limiting the antimicrobial efficacy by solely relying on its sharp edges. Furthermore, achieving a significant antimicrobial effect solely through MXene's sharp edges requires a high concentration of the material. The abundance of functional groups and hydrophilicity of the MXene nanosheets enhance their contact efficiency with bacteria. Subsequently, the sharp edges of MXene nanosheets disrupt the bacterial cell walls, leading to cytoplasmic leakage and bacterial DNA release. Additionally, hydrogen bonds between oxygenated groups on MXene's surface and lipopolysaccharides on bacterial membranes restrict nutrient intake by bacteria. Rasool *et al.* first proposed MXene's antimicrobial mechanism as a ‘Nano-Knife’, showing significant inhibitory effects of Ti<sub>3</sub>C<sub>2</sub>T<sub>x</sub> nanosheets against both Gram-negative *E. coli* and Gram-positive *Bacillus subtilis*.<sup>43</sup> Their findings, based on scanning electron microscopy, transmission microscopy images, glutathione (GSH) oxidation analysis, and lactate dehydrogenase release (LDH) analysis, suggested that MXene's antimicrobial mechanism involves sharp edge-induced cell wall rupture and oxidative stress from electron transfer. Using techniques such as flow cytometry, fluorescence imaging, and broth microdilution assays, Shamsabadi *et al.* elucidated the damage caused to bacterial cell walls by MXene's sharp edges and confirmed the MXene's size- and exposure time-dependent antimicrobial activity.

### 7.2. ROS generator mechanism

Due to their abundant electronic properties, MXenes possess the capability to eradicate bacteria by inducing cytotoxic ROS and oxidative stress upon photoexcitation.<sup>43</sup> Under light excitation, MXene serves as a photosensitizer, transferring energy to



Table 2 Comparison of antibacterial activity of non-Ti MXenes based on recent reports

Material	Technique	Mechanism	Bacterial strain	Application	Ref.
Nb <sub>2</sub> CT <sub>x</sub> , Nb <sub>4</sub> C <sub>3</sub> T <sub>x</sub>	—	Oxidative stress	<i>Escherichia coli</i> , <i>Staphylococcus aureus</i>	—	88
Nb <sub>2</sub> CT <sub>x</sub> @TP	Photothermal transduction	ROS generation	<i>Escherichia coli</i> , <i>Staphylococcus aureus</i>	Bacterial Infection elimination, tissue regeneration	90
Nb <sub>2</sub> CT <sub>x</sub> @PDA	ROS/temperature dual-responsive therapy	ROS generation	<i>Escherichia coli</i> , <i>Staphylococcus aureus</i> , MRSA	MRSA-infected wound healing	92
Nb <sub>2</sub> CT <sub>x</sub> @Gel system (Nb <sub>2</sub> C and Gel = PLGA-PEG-PLGA triblock copolymer)	NIR (II) photothermal activity	ROS scavenging	<i>Staphylococcus aureus</i> , <i>Escherichia coli</i>	Diabetic wound healing	93
CeO <sub>2</sub> /Nb <sub>2</sub> CT <sub>x</sub> nanozyme	Photothermal anti-bacterial activity	Fenton reaction	MRSA	Diabetic wound infection	94
Nb <sub>2</sub> CT <sub>x</sub> and Nb <sub>4</sub> C <sub>3</sub> T <sub>x</sub> modified with lysozyme	—	ROS generation	<i>Bacillus subtilis</i> , <i>Staphylococcus aureus</i>	—	89
Porphyrin MOF-Nb <sub>2</sub> CT <sub>x</sub>	Sonodynamic therapy	ATP synthesis, ROS generation	MRSA	Antibacterial therapy and bone regeneration	91
MoO <sub>x</sub> @Mo <sub>2</sub> CT <sub>x</sub>	Sonocatalytic therapy	ROS generation	<i>Escherichia coli</i> , <i>Staphylococcus aureus</i> , MRSA	Bacterial eradication	95
BODIPY-Mo <sub>2</sub> CT <sub>x</sub>	Photothermal and photodynamic effects	ROS generation	<i>Escherichia coli</i> , <i>Staphylococcus aureus</i>	—	96
V <sub>2</sub> CT <sub>x</sub> nanosheets	Photothermal therapy	ROS production	<i>Escherichia coli</i> , <i>Staphylococcus aureus</i>	—	97
V <sub>2</sub> CT <sub>x</sub>	Photothermal activity	Breakage of cell wall	<i>Escherichia coli</i> , <i>Staphylococcus aureus</i>	Sterilization applications	98
4 K10@V <sub>2</sub> CT <sub>x</sub>	Photothermal effect	ROS generation, disruption of the cell wall by “Nanoblade effect”	MRSA, Methicillin-resistant <i>Staphylococcus epidermidis</i> (MRSE), <i>Pseudomonas aeruginosa</i> , <i>Escherichia coli</i>	Microneedle array for photo-excited bacteria-killing	99
V <sub>2</sub> NT <sub>x</sub> nanozyme	Photothermal effect	ROS generation, enzymatic activity	<i>Staphylococcus aureus</i> , <i>Streptococcus mutans</i>	Anti-infective therapy	102
V <sub>2</sub> CT <sub>x</sub> nanosheet-based nanozyme	—	ROS production	<i>Escherichia coli</i> , <i>Staphylococcus aureus</i>	Colorimetric sensing	100
Pt@V <sub>2</sub> CT <sub>x</sub>	“Nanozyme” effect with photothermal and chemodynamic therapy	Enzyme-like activity	MRSA	Against bacterial keratitis	101
TiVCT <sub>x</sub>	“Nanoknife” effect + NIR laser	Nanoknife effect	<i>Escherichia coli</i>	Sterilization application	103

### MXene's Antibacterial Activity – Mode of Action

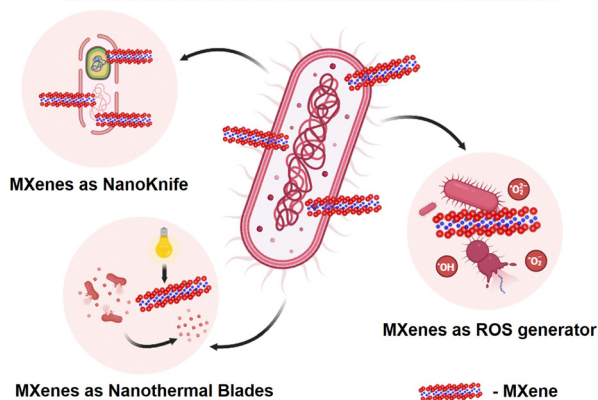


Fig. 8 Schematic representation showing the different mechanisms of the MXene's antibacterial activity.

oxygen (O<sub>2</sub>) or water (H<sub>2</sub>O) to produce ROS, such as singlet oxygen (<sup>1</sup>O<sub>2</sub>), hydroxyl radicals (\*OH), and superoxide radicals

(O<sub>2</sub><sup>-</sup>). The generation of ROS is intricately linked to the intrinsic structure of MXenes, including factors such as the number of MXene layers, stacking mode, sizes, doping, and defects. Density functional theory (DFT) calculations reveal that surface terminations and modifications of MXenes can significantly alter their mechanical, optical, and electrical properties, consequently affecting their redox capabilities and ROS generation potential.<sup>104</sup> Excessive ROS typically induce cellular oxidative stress in microbes, which leads to mitochondrial dysfunction by causing oxidative damage to biomacromolecules and cell membranes, ultimately resulting in cell death. The reduced activity of superoxide dismutase (SOD), a crucial antioxidant enzyme, in MXene-exposed bacteria may account for the heightened intracellular ROS levels and ensuing oxidative damage, as evidenced by measurements of intracellular ROS levels and SOD activity.<sup>105</sup> Moreover, the elevated production of malondialdehyde (MDA), a lipid peroxidation product indicating cell membrane damage, in MXene-exposed bacterial cells further confirms the oxidative harm inflicted by MXene-generated ROS on bacterial membranes.



### 7.3. Nanothermal blade mechanism

The exceptional localized surface plasmon resonance (LSPR) effects of MXene, attributed to its large specific surface area, abundant free electron distribution, and broad-spectrum absorption, render it a promising photothermal agent. MXenes exhibit remarkable photothermal conversion efficiency, which generates heat and ROS upon laser irradiation, leading to bacterial inactivation.<sup>105</sup> The heat produced profoundly impacts cellular structures and substances, such as cell walls, nucleic acids, and proteins, effectively inhibiting bacterial metabolic activities. Consequently, MXene has earned the name “nanothermal blade” due to its remarkable photothermal properties and sharp edges.<sup>106</sup> Furthermore, thermotherapy has been shown to enhance the permeability of pathogenic microorganism membranes, thereby augmenting the antibacterial penetration of ROS or metal ions.

## 8. Conclusion and future perspectives

Based on the current evidence, we can clearly say that non-Ti MXenes emerge as a great alternative for Ti MXenes due to their high biocompatibility, biodegradability and efficiency. Apart from their antibacterial and nanozyme activities, non-Ti MXenes have a plethora of applications in the field of biomedicine, including drug delivery, photothermal therapy, chemodynamic therapy and sonodynamic therapy. The nanozyme activity enables the MXene to scavenge the ROS that is implicated in many degenerative diseases. Simultaneously, these MXenes elicit their antibacterial activity by creating ROS in bacterial cells and by acting as nanoknives. Apart from therapeutics, the unique properties of non-Ti MXenes enable their use in diagnosis as sensors and imaging agents. This makes non-Ti MXenes excellent candidates for theranostics. Compared to the Ti-based MXenes, the non-Ti MXene alternatives are significantly biocompatible and biodegradable; hence, non-Ti MXenes are better candidates for biomedical applications than Ti MXenes. Further studies will open new horizons for the development of novel therapeutic and theranostic strategies based on these materials.

Various approaches can be employed to improve MXenes for biological applications. Enhancing the biocompatibility will help in the possible clinical translation of MXene-based therapeutic strategies. Biocompatibility can be improved by surface functionalisation, functionalising with biocompatible polymers or biomolecules helps in reducing toxicity and immunogenicity. The stability of MXenes can be increased by refining the synthesis process to generate more chemically stable MXenes to prevent their oxidation or rapid degradation in biological environments. Enhancing the specificity and effectiveness of cancer therapy, and biosensing can be accomplished by the addition of targeted ligands, medicines, or imaging agents. Furthermore, extensive *in vivo* investigations are essential for comprehending the pharmacokinetics, bio distribution, and long-term impacts of these materials to guarantee their safe and efficient application in clinical settings. Through multidisciplinary

research, we can substantially improve the use of MXenes for biomedical applications.

However, numerous significant challenges are yet to be addressed. The scalability of non-Ti MXenes is constrained by the limited availability of precursor MAX phases and dependence on difficult etching techniques.<sup>107</sup> Moreover, the long-term biological effects, encompassing pharmacokinetics, bio-distribution, and possible off-target effects remain inadequately studied. The proposed solutions, such as surface functionalization with biopolymers or targeted ligands, are promising, and they may unintentionally raise synthesis complexity and vary the inherent properties of the material. Similarly, improving the stability by altered synthesis techniques may affect other advantageous characteristics, such as biodegradability, perhaps resulting in unforeseen effects in *in vivo* experiments. To bridge the disparity between experimental potential and clinical application, enhanced *in vivo* investigations and interdisciplinary collaboration are imperative. This encompasses a thorough understanding of toxicity, immunological reactions, and prolonged effects across diverse biological conditions. Although non-Ti MXenes possess considerable potential, their therapeutic applicability depends on surmounting these substantial obstacles through innovation and careful validation.

## Author contributions

The manuscript was written through contributions of all authors. All authors have given approval to the final version of the manuscript.

## Data availability

Data sharing is not applicable to this article as no datasets were generated or analysed during the current study.

## Conflicts of interest

The authors declare no conflicts of interest.

## Acknowledgements

PAR acknowledges Ramalingaswami re-entry fellowship (BT/RLF/Re-entry/75/2020) from the Department of Biotechnology (DBT), Govt. of India. The authors acknowledge CSR funding from Higher Education Financing Agency (HEFA), Bengaluru, India (SAN/CSR/17/2023-24). VGG acknowledges the Indian Institute of Technology Palakkad and MHRD, Govt. of India for funding.

## References

- 1 K. Rasool, R. P. Pandey, P. A. Rasheed, S. Buczek, Y. Gogotsi and K. A. Mahmoud, Water treatment and environmental remediation applications of two-dimensional



- metal carbides (MXenes), *Mater. Today*, 2019, **30**, 80–102, DOI: [10.1016/j.mattod.2019.05.017](https://doi.org/10.1016/j.mattod.2019.05.017).
- 2 L. Gao, Y. Zhao, X. Chang, J. Zhang, Y. Li, S. Wageh, O. A. Al-Hartomy, A. G. Al-Sehemi, H. Zhang and H. Ågren, Emerging applications of MXenes for photodetection: Recent advances and future challenges, *Mater. Today*, 2022, **61**, 169–190, DOI: [10.1016/j.mattod.2022.10.022](https://doi.org/10.1016/j.mattod.2022.10.022).
  - 3 L. Chen, X. Dai, W. Feng and Y. Chen, Biomedical Applications of MXenes: From Nanomedicine to Biomaterials, *Acc. Mater. Res.*, 2022, **3**(8), 785–798, DOI: [10.1021/account.smr.2c00025](https://doi.org/10.1021/account.smr.2c00025).
  - 4 D. H. Ho, Y. Y. Choi, S. B. Jo, J.-M. Myoung and J. H. Cho, Sensing with MXenes: Progress and Prospects, *Adv. Mater.*, 2021, **33**(47), 2005846, DOI: [10.1002/adma.202005846](https://doi.org/10.1002/adma.202005846).
  - 5 H. Kim and H. N. Alshareef, MXetronics: MXene-Enabled Electronic and Photonic Devices, *ACS Mater. Lett.*, 2020, **2**(1), 55–70, DOI: [10.1021/acsmaterialslett.9b00419](https://doi.org/10.1021/acsmaterialslett.9b00419).
  - 6 B. Anasori, M. R. Lukatskaya and Y. Gogotsi, 2D metal carbides and nitrides (MXenes) for energy storage, *Nat. Rev. Mater.*, 2017, **2**(2), 16098, DOI: [10.1038/natrevmats.2016.98](https://doi.org/10.1038/natrevmats.2016.98).
  - 7 M. Naguib, M. Kurtoglu, V. Presser, J. Lu, J. Niu, M. Heon, L. Hultman, Y. Gogotsi and M. W. Barsoum, Two-Dimensional Nanocrystals Produced by Exfoliation of Ti<sub>3</sub>AlC<sub>2</sub>, *Adv. Mater.*, 2011, **23**(37), 4248–4253, DOI: [10.1002/adma.201102306](https://doi.org/10.1002/adma.201102306).
  - 8 A. Feng, Y. Yu, Y. Wang, F. Jiang, Y. Yu, L. Mi and L. Song, Two-dimensional MXene Ti<sub>3</sub>C<sub>2</sub> produced by exfoliation of Ti<sub>3</sub>AlC<sub>2</sub>, *Mater. Des.*, 2017, **114**, 161–166, DOI: [10.1016/j.matdes.2016.10.053](https://doi.org/10.1016/j.matdes.2016.10.053).
  - 9 K. Wang, Y. Zhou, W. Xu, D. Huang, Z. Wang and M. Hong, Fabrication and thermal stability of two-dimensional carbide Ti<sub>3</sub>C<sub>2</sub> nanosheets, *Ceram. Int.*, 2016, **42**(7), 8419–8424, DOI: [10.1016/j.ceramint.2016.02.059](https://doi.org/10.1016/j.ceramint.2016.02.059).
  - 10 C. E. Shuck, M. Han, K. Maleski, K. Hantanasirisakul, S. J. Kim, J. Choi, W. E. B. Reil and Y. Gogotsi, Effect of Ti<sub>3</sub>AlC<sub>2</sub> MAX Phase on Structure and Properties of Resultant Ti<sub>3</sub>C<sub>2</sub>T<sub>x</sub> MXene, *ACS Appl. Nano Mater.*, 2019, **2**(6), 3368–3376, DOI: [10.1021/acsnm.9b00286](https://doi.org/10.1021/acsnm.9b00286).
  - 11 Y. Tian, W. Que, Y. Luo, C. Yang, X. Yin and L. B. Kong, Surface nitrogen-modified 2D titanium carbide (MXene) with high energy density for aqueous supercapacitor applications, *J. Mater. Chem. A*, 2019, **7**(10), 5416–5425, DOI: [10.1039/C9TA00076C](https://doi.org/10.1039/C9TA00076C).
  - 12 M. Li, J. Lu, K. Luo, Y. Li, K. Chang, K. Chen, J. Zhou, J. Rosen, L. Hultman and P. Eklund, *et al.*, Element Replacement Approach by Reaction with Lewis Acidic Molten Salts to Synthesize Nanolaminated MAX Phases and MXenes, *J. Am. Chem. Soc.*, 2019, **141**(11), 4730–4737, DOI: [10.1021/jacs.9b00574](https://doi.org/10.1021/jacs.9b00574).
  - 13 L. Verger, C. Xu, V. Nату, H.-M. Cheng, W. Ren and M. W. Barsoum, Overview of the synthesis of MXenes and other ultrathin 2D transition metal carbides and nitrides, *Curr. Opin. Solid State Mater. Sci.*, 2019, **23**(3), 149–163, DOI: [10.1016/j.cossms.2019.02.001](https://doi.org/10.1016/j.cossms.2019.02.001).
  - 14 W. Sun, S. A. Shah, Y. Chen, Z. Tan, H. Gao, T. Habib, M. Radovic and M. J. Green, Electrochemical etching of Ti<sub>2</sub>AlC to Ti<sub>2</sub>CT<sub>x</sub> (MXene) in low-concentration hydrochloric acid solution, *J. Mater. Chem. A*, 2017, **5**(41), 21663–21668, DOI: [10.1039/C7TA05574A](https://doi.org/10.1039/C7TA05574A).
  - 15 Y. Li, H. Shao, Z. Lin, J. Lu, L. Liu, B. Duployer, P. O. Å. Persson, P. Eklund, L. Hultman and M. Li, *et al.*, A general Lewis acidic etching route for preparing MXenes with enhanced electrochemical performance in non-aqueous electrolyte, *Nat. Mater.*, 2020, **19**(8), 894–899, DOI: [10.1038/s41563-020-0657-0](https://doi.org/10.1038/s41563-020-0657-0).
  - 16 Y.-J. Kim, S. J. Kim, D. Seo, Y. Chae, M. Anayee, Y. Lee, Y. Gogotsi, C. W. Ahn and H.-T. Jung, Etching Mechanism of Monoatomic Aluminum Layers during MXene Synthesis, *Chem. Mater.*, 2021, **33**(16), 6346–6355, DOI: [10.1021/acs.chemmater.1c01263](https://doi.org/10.1021/acs.chemmater.1c01263).
  - 17 D. Wang, C. Zhou, A. S. Filatov, W. Cho, F. Lagunas, M. Wang, S. Vaikuntanathan, C. Liu, R. F. Klie and D. V. Talapin, Direct synthesis and chemical vapor deposition of 2D carbide and nitride MXenes, *Science*, 2023, **379**(6638), 1242–1247.
  - 18 S.-Y. Pang, Y.-T. Wong, S. Yuan, Y. Liu, M.-K. Tsang, Z. Yang, H. Huang, W.-T. Wong and J. Hao, Universal Strategy for HF-Free Facile and Rapid Synthesis of Two-dimensional MXenes as Multifunctional Energy Materials, *J. Am. Chem. Soc.*, 2019, **141**(24), 9610–9616, DOI: [10.1021/jacs.9b02578](https://doi.org/10.1021/jacs.9b02578).
  - 19 X. Li, M. Li, Q. Yang, G. Liang, Z. Huang, L. Ma, D. Wang, F. Mo, B. Dong and Q. Huang, *et al.*, In Situ Electrochemical Synthesis of MXenes without Acid/Alkali Usage in/for an Aqueous Zinc Ion Battery, *Adv. Energy Mater.*, 2020, **10**(36), 2001791, DOI: [10.1002/aenm.202001791](https://doi.org/10.1002/aenm.202001791).
  - 20 G. P. Lim, C. F. Soon, N. L. Ma, M. Morsin, N. Nayan, M. K. Ahmad and K. S. Tee, Cytotoxicity of MXene-based nanomaterials for biomedical applications: A mini review, *Environ. Res.*, 2021, **201**, 111592, DOI: [10.1016/j.envres.2021.111592](https://doi.org/10.1016/j.envres.2021.111592).
  - 21 S. S. Siwal, H. Kaur, G. Chauhan and V. K. Thakur, MXene-Based Nanomaterials for Biomedical Applications: Healthier Substitute Materials for the Future, *Adv. NanoBiomed Res.*, 2023, **3**(1), 2200123, DOI: [10.1002/anbr.202200123](https://doi.org/10.1002/anbr.202200123).
  - 22 K. Huang, Z. Li, J. Lin, G. Han and P. Huang, Two-dimensional transition metal carbides and nitrides (MXenes) for biomedical applications, *Chem. Soc. Rev.*, 2018, **47**(14), 5109–5124, DOI: [10.1039/C7CS00838D](https://doi.org/10.1039/C7CS00838D).
  - 23 Y. Lai, C. Zhou, P. Huang, Z. Dong, C. Mo, L. Xie, H. Lin, Z. Zhou, G. Deng and Y. Liu, *et al.*, Polydatin alleviated alcoholic liver injury in zebrafish larvae through ameliorating lipid metabolism and oxidative stress, *J. Pharmacol. Sci.*, 2018, **138**, DOI: [10.1016/j.jphs.2018.08.007](https://doi.org/10.1016/j.jphs.2018.08.007).
  - 24 A. Szuplewska, D. Kulpińska, M. Jakubczak, A. Dybko, M. Chudy, A. Olszyna, Z. Brzózka and A. M. Jastrzębska, The 10th anniversary of MXenes: Challenges and prospects for their surface modification toward future biotechnological applications, *Adv. Drug Delivery Rev.*, 2022, **182**, 114099, DOI: [10.1016/j.addr.2021.114099](https://doi.org/10.1016/j.addr.2021.114099).
  - 25 F. Shahzad, M. Alhabeab, C. B. Hatter, B. Anasori, S. Man Hong, C. M. Koo and Y. Gogotsi, Electromagnetic



- interference shielding with 2D transition metal carbides (MXenes, *Science*, 2016, 353(6304), 1137–1140, DOI: [10.1126/science.aag2421](https://doi.org/10.1126/science.aag2421).
- 26 X. Han, J. Huang, H. Lin, Z. Wang, P. Li and Y. Chen, 2D Ultrathin MXene-Based Drug-Delivery NanoplatforM for Synergistic Photothermal Ablation and Chemotherapy of Cancer, *Adv. Healthcare Mater.*, 2018, 7(9), 1701394, DOI: [10.1002/adhm.201701394](https://doi.org/10.1002/adhm.201701394).
- 27 Y. Liu, Q. Han, W. Yang, X. Gan, Y. Yang, K. Xie, L. Xie and Y. Deng, Two-dimensional MXene/cobalt nanowire hetero-junction for controlled drug delivery and chemo-photo-thermal therapy, *Mater. Sci. Eng., C*, 2020, 116, 111212, DOI: [10.1016/j.msec.2020.111212](https://doi.org/10.1016/j.msec.2020.111212).
- 28 M. Khazaei, M. Arai, T. Sasaki, C.-Y. Chung, N. S. Venkataramanan, M. Estili, Y. Sakka and Y. Kawazoe, Novel Electronic and Magnetic Properties of Two-Dimensional Transition Metal Carbides and Nitrides, *Adv. Funct. Mater.*, 2013, 23(17), 2185–2192, DOI: [10.1002/adfm.201202502](https://doi.org/10.1002/adfm.201202502).
- 29 J. Xuan, Z. Wang, Y. Chen, D. Liang, L. Cheng, X. Yang, Z. Liu, R. Ma, T. Sasaki and F. Geng, Organic-Base-Driven Intercalation and Delamination for the Production of Functionalized Titanium Carbide Nanosheets with Superior Photothermal Therapeutic Performance, *Angew. Chem., Int. Ed.*, 2016, 55(47), 14569–14574, DOI: [10.1002/anie.201606643](https://doi.org/10.1002/anie.201606643).
- 30 H. Lin, S. Gao, C. Dai, Y. Chen and J. Shi, A Two-Dimensional Biodegradable Niobium Carbide (MXene) for Photothermal Tumor Eradication in NIR-I and NIR-II Biowindows, *J. Am. Chem. Soc.*, 2017, 139(45), 16235–16247, DOI: [10.1021/jacs.7b07818](https://doi.org/10.1021/jacs.7b07818).
- 31 X. Wang, Y. Ma, X. Sheng, Y. Wang and H. Xu, Ultrathin Polypyrrole Nanosheets via Space-Confined Synthesis for Efficient Photothermal Therapy in the Second Near-Infrared Window, *Nano Lett.*, 2018, 18(4), 2217–2225, DOI: [10.1021/acs.nanolett.7b04675](https://doi.org/10.1021/acs.nanolett.7b04675).
- 32 R. B. Rakhi, P. Nayak, C. Xia and H. N. Alshareef, Erratum: Novel amperometric glucose biosensor based on MXene nanocomposite, *Sci. Rep.*, 2016, 6(1), 38465, DOI: [10.1038/srep38465](https://doi.org/10.1038/srep38465).
- 33 L. Wu, Q. You, Y. Shan, S. Gan, Y. Zhao, X. Dai and Y. Xiang, Few-layer  $\text{Ti}_3\text{C}_2\text{T}_x$  MXene: A promising surface plasmon resonance biosensing material to enhance the sensitivity, *Sens. Actuators, B*, 2018, 277, 210–215, DOI: [10.1016/j.snb.2018.08.154](https://doi.org/10.1016/j.snb.2018.08.154).
- 34 L. Wu, X. Yuan, Y. Tang, S. Wageh, O. A. Al-Hartomy, A. G. Al-Sehemi, J. Yang, Y. Xiang, H. Zhang and Y. Qin, MXene sensors based on optical and electrical sensing signals: from biological, chemical, and physical sensing to emerging intelligent and bionic devices, *Photonix*, 2023, 4(1), 15, DOI: [10.1186/s43074-023-00091-7](https://doi.org/10.1186/s43074-023-00091-7).
- 35 S. K. Bhardwaj, H. Singh, M. Khatri, K.-H. Kim and N. Bhardwaj, Advances in MXenes-based optical biosensors: A review, *Biosens. Bioelectron.*, 2022, 202, 113995, DOI: [10.1016/j.bios.2022.113995](https://doi.org/10.1016/j.bios.2022.113995).
- 36 B. Xu, C. Zhi and P. Shi, Latest advances in MXene biosensors, *J. Phys. Mater.*, 2020, 3(3), 031001, DOI: [10.1088/2515-7639/ab8f78](https://doi.org/10.1088/2515-7639/ab8f78).
- 37 H. Lin, Y. Chen and J. Shi, Insights into 2D MXenes for Versatile Biomedical Applications: Current Advances and Challenges Ahead, *Adv. Sci.*, 2018, 5(10), 1800518, DOI: [10.1002/advs.201800518](https://doi.org/10.1002/advs.201800518).
- 38 Z. Xie, S. Chen, Y. Duo, Y. Zhu, T. Fan, Q. Zou, M. Qu, Z. Lin, J. Zhao and Y. Li, *et al.*, Biocompatible Two-Dimensional Titanium Nanosheets for Multimodal Imaging-Guided Cancer Theranostics, *ACS Appl. Mater. Interfaces*, 2019, 11(25), 22129–22140, DOI: [10.1021/acsami.9b04628](https://doi.org/10.1021/acsami.9b04628).
- 39 B. Gürbüz and F. Ciftci, Bio-electric-electronics and tissue engineering applications of MXenes wearable materials: A review, *Chem. Eng. J.*, 2024, 489, 151230, DOI: [10.1016/j.cej.2024.151230](https://doi.org/10.1016/j.cej.2024.151230).
- 40 M. S. Kang, H. J. Jang, H. J. Jo, I. S. Raja and D.-W. Han, MXene and Xene: promising frontier beyond graphene in tissue engineering and regenerative medicine, *Nanoscale Horiz.*, 2024, 9(1), 93–117, DOI: [10.1039/D3NH00428G](https://doi.org/10.1039/D3NH00428G).
- 41 B. C. Wyatt, A. Rosenkranz and B. Anasori, 2D MXenes: Tunable Mechanical and Tribological Properties, *Adv. Mater.*, 2021, 33(17), 2007973, DOI: [10.1002/adma.202007973](https://doi.org/10.1002/adma.202007973).
- 42 A. Arabi Shamsabadi, M. Sharifian Gh, B. Anasori and M. Soroush, Antimicrobial Mode-of-Action of Colloidal  $\text{Ti}_3\text{C}_2\text{T}_x$  MXene Nanosheets, *ACS Sustainable Chem. Eng.*, 2018, 6(12), 16586–16596, DOI: [10.1021/acssuschemeng.8b03823](https://doi.org/10.1021/acssuschemeng.8b03823).
- 43 K. Rasool, M. Helal, A. Ali, C. E. Ren, Y. Gogotsi and K. A. Mahmoud, Antibacterial Activity of  $\text{Ti}_3\text{C}_2\text{T}_x$  MXene, *ACS Nano*, 2016, 10(3), 3674–3684, DOI: [10.1021/acsnano.6b00181](https://doi.org/10.1021/acsnano.6b00181).
- 44 M. Ozkan, MXenes vs. MBenes: Demystifying the materials of tomorrow's carbon capture revolution, *MRS Energy Sustainability*, 2024, 11(1), 181–190, DOI: [10.1557/s43581-024-00082-6](https://doi.org/10.1557/s43581-024-00082-6).
- 45 B. C. Wyatt, S. K. Nemani, K. Desai, H. Kaur, B. Zhang and B. Anasori, High-temperature stability and phase transformations of titanium carbide ( $\text{Ti}_3\text{C}_2\text{T}_x$ ) MXene, *J. Phys.: Condens. Matter*, 2021, 33(22), 224002, DOI: [10.1088/1361-648X/abe793](https://doi.org/10.1088/1361-648X/abe793).
- 46 Y. Wen, L. Hu, J. Li, Y. Geng, Y. Yang, J. Wang, X. Chen, L. Yu, H. Tang and T. Han, *et al.*, Exposure to two-dimensional ultrathin  $\text{Ti}_3\text{C}_2$  (MXene) nanosheets during early pregnancy impairs neurodevelopment of offspring in mice, *J. Nanobiotechnol.*, 2022, 20(1), 108, DOI: [10.1186/s12951-022-01313-z](https://doi.org/10.1186/s12951-022-01313-z).
- 47 Y. Wei, R. Bao, L. Hu, Y. Geng, X. Chen, Y. Wen, Y. Wang, M. Qin, Y. Zhang and X. Liu,  $\text{Ti}_3\text{C}_2$  (MXene) nanosheets disrupt spermatogenesis in male mice mediated by the ATM/p53 signaling pathway, *Biol. Direct*, 2023, 18(1), 30, DOI: [10.1186/s13062-023-00382-w](https://doi.org/10.1186/s13062-023-00382-w).
- 48 W. Wu, H. Ge, L. Zhang, X. Lei, Y. Yang, Y. Fu and H. Feng, Evaluating the Cytotoxicity of  $\text{Ti}_3\text{C}_2$  MXene to Neural Stem Cells, *Chem. Res. Toxicol.*, 2020, 33(12), 2953–2962, DOI: [10.1021/acs.chemrestox.0c00232](https://doi.org/10.1021/acs.chemrestox.0c00232).
- 49 M. Naguib, J. Halim, J. Lu, K. M. Cook, L. Hultman, Y. Gogotsi and M. W. Barsoum, New Two-Dimensional



- Niobium and Vanadium Carbides as Promising Materials for Li-Ion Batteries, *J. Am. Chem. Soc.*, 2013, **135**(43), 15966–15969, DOI: [10.1021/ja405735d](https://doi.org/10.1021/ja405735d).
- 50 P. A. Rasheed, R. P. Pandey, F. Banat and S. W. Hasan, Recent advances in niobium MXenes: Synthesis, properties, and emerging applications, *Matter*, 2022, **5**(2), 546–572, DOI: [10.1016/j.matt.2021.12.021](https://doi.org/10.1016/j.matt.2021.12.021).
- 51 C. Lamiel, I. Hussain, J. H. Warner and K. Zhang, Beyond Ti-based MXenes: A review of emerging non-Ti based metal-MXene structure, properties, and applications, *Mater. Today*, 2023, **63**, 313–338, DOI: [10.1016/j.mattod.2023.01.020](https://doi.org/10.1016/j.mattod.2023.01.020).
- 52 I. Hussain, U. Amara, F. Bibi, A. Hanan, M. N. Lakhan, I. A. Soomro, A. Khan, I. Shaheen, U. Sajjad and G. Mohana Rani, *et al.*, Mo-based MXenes: Synthesis, properties, and applications, *Adv. Colloid Interface Sci.*, 2024, **324**, 103077, DOI: [10.1016/j.cis.2023.103077](https://doi.org/10.1016/j.cis.2023.103077).
- 53 A. M. Jastrzębska, B. Scheibe, A. Szuplewska, A. Rozmysłowska-Wojciechowska, M. Chudy, C. Aparicio, M. Scheibe, I. Janica, A. Ciesielski and M. Otyepka, *et al.*, On the rapid in situ oxidation of two-dimensional V<sub>2</sub>C<sub>7</sub>T<sub>z</sub> MXene in culture cell media and their cytotoxicity, *Mater. Sci. Eng., C*, 2021, **119**, 111431, DOI: [10.1016/j.msec.2020.111431](https://doi.org/10.1016/j.msec.2020.111431).
- 54 L. Fusco, A. Gazzì, C. E. Shuck, M. Orecchioni, D. Alberti, S. M. D'Almeida, D. Rinchai, E. Ahmed, O. Elhanani and M. Rauner, *et al.*, Immune Profiling and Multiplexed Label-Free Detection of 2D MXenes by Mass Cytometry and High-Dimensional Imaging, *Adv. Mater.*, 2022, **34**(45), 2205154, DOI: [10.1002/adma.202205154](https://doi.org/10.1002/adma.202205154).
- 55 G. Yang, J. Zhao, S. Yi, X. Wan and J. Tang, Biodegradable and photostable Nb<sub>2</sub>C MXene quantum dots as promising nanofluorophores for metal ions sensing and fluorescence imaging, *Sens. Actuators, B*, 2020, **309**, 127735, DOI: [10.1016/j.snb.2020.127735](https://doi.org/10.1016/j.snb.2020.127735).
- 56 M. Gu, Z. Dai, X. Yan, J. Ma, Y. Niu, W. Lan, X. Wang and Q. Xu, Comparison of toxicity of Ti<sub>3</sub>C<sub>2</sub> and Nb<sub>2</sub>C MXene quantum dots (QDs) to human umbilical vein endothelial cells, *J. Appl. Toxicol.*, 2021, **41**(5), 745–754, DOI: [10.1002/jat.4085](https://doi.org/10.1002/jat.4085).
- 57 W. Feng, R. Wang, Y. Zhou, L. Ding, X. Gao, B. Zhou, P. Hu and Y. Chen, Ultrathin Molybdenum Carbide MXene with Fast Biodegradability for Highly Efficient Theory-Oriented Photonic Tumor Hyperthermia, *Adv. Funct. Mater.*, 2019, **29**(22), 1901942, DOI: [10.1002/adfm.201901942](https://doi.org/10.1002/adfm.201901942).
- 58 L. Fusco, A. Gazzì, C. E. Shuck, M. Orecchioni, E. I. Ahmed, L. Giro, B. Zavan, A. Yilmazer, K. Ley and D. Bedognetti, *et al.*, V<sub>4</sub>C<sub>3</sub> MXene Immune Profiling and Modulation of T Cell-Dendritic Cell Function and Interaction, *Small Methods*, 2023, **7**(8), 2300197, DOI: [10.1002/smt.202300197](https://doi.org/10.1002/smt.202300197).
- 59 A. P. Singh, A. Biswas, A. Shukla and P. Maiti, Targeted therapy in chronic diseases using nanomaterial-based drug delivery vehicles, *Signal Transduction Targeted Ther.*, 2019, **4**(1), 33, DOI: [10.1038/s41392-019-0068-3](https://doi.org/10.1038/s41392-019-0068-3).
- 60 S. Patnaik, B. Gorain, S. Padhi, H. Choudhury, G. A. Gabr, S. Md, D. Kumar Mishra and P. Kesharwani, Recent update of toxicity aspects of nanoparticulate systems for drug delivery, *Eur. J. Pharm. Biopharm.*, 2021, **161**, 100–119, DOI: [10.1016/j.ejpb.2021.02.010](https://doi.org/10.1016/j.ejpb.2021.02.010).
- 61 P. Parhi, C. Mohanty and S. K. Sahoo, Nanotechnology-based combinational drug delivery: an emerging approach for cancer therapy, *Drug Discovery Today*, 2012, **17**(17), 1044–1052, DOI: [10.1016/j.drudis.2012.05.010](https://doi.org/10.1016/j.drudis.2012.05.010).
- 62 X. Chang, Q. Wu, Y. Wu, X. Xi, J. Cao, H. Chu, Q. Liu, Y. Li, W. Wu and X. Fang, *et al.*, Multifunctional Au Modified Ti<sub>3</sub>C<sub>2</sub>-MXene for Photothermal/Enzyme Dynamic/Immune Synergistic Therapy, *Nano Lett.*, 2022, **22**(20), 8321–8330, DOI: [10.1021/acs.nanolett.2c03260](https://doi.org/10.1021/acs.nanolett.2c03260).
- 63 S. S. Sana, M. Santhamoorthy, R. Haldar, C. J. Raorane, S. Irvani, R. S. Varma and S.-C. Kim, Recent advances on MXene-based hydrogels for antibacterial and drug delivery applications, *Process Biochem.*, 2023, **132**, 200–220, DOI: [10.1016/j.procbio.2023.06.022](https://doi.org/10.1016/j.procbio.2023.06.022).
- 64 Z. Hao, Y. Li, X. Liu, T. Jiang, Y. He, X. Zhang, C. Cong, D. Wang, Z. Liu and D. Gao, Enhancing biocatalysis of a MXene-based biomimetic plasmonic assembly for targeted cancer treatments in NIR-II biowindow, *Chem. Eng. J.*, 2021, **425**, 130639, DOI: [10.1016/j.cej.2021.130639](https://doi.org/10.1016/j.cej.2021.130639).
- 65 X. Han, X. Jing, D. Yang, H. Lin, Z. Wang, H. Ran, P. Li and Y. Chen, Therapeutic mesopore construction on 2D Nb<sub>2</sub>C MXenes for targeted and enhanced chemo-photothermal cancer therapy in NIR-II biowindow, *Theranostics*, 2018, **8**(16), 4491–4508.
- 66 Y. Lu, X. Zhang, X. Hou, M. Feng, Z. Cao and J. Liu, Functionalized 2D Nb<sub>2</sub>C nanosheets for primary and recurrent cancer photothermal/immune-therapy in the NIR-II biowindow, *Nanoscale*, 2021, **13**(42), 17822–17836, DOI: [10.1039/D1NR05126A](https://doi.org/10.1039/D1NR05126A).
- 67 B. Richard, C. Shahana, R. Vivek, M. Amarendar Reddy and P. A. Rasheed, Acoustic platforms meet MXenes – a new paradigm shift in the palette of biomedical applications, *Nanoscale*, 2023, **15**(45), 18156–18172, DOI: [10.1039/D3NR04901A](https://doi.org/10.1039/D3NR04901A).
- 68 E. Pang, B. Li, C. Zhou, S. Zhao, Y. Tang, Q. Tan, C. Yao, B. Wang, K. Han and X. Song, *et al.*, Catalase-like pleated niobium carbide MXene loaded with polythiophene for oxygenated sonodynamic therapy in solid tumor, *Nanoscale*, 2023, **15**(40), 16466–16471, DOI: [10.1039/D3NR03731B](https://doi.org/10.1039/D3NR03731B).
- 69 A. Jastrzebska, A. Szuplewska, A. Rozmysłowska-Wojciechowska, J. Mitrzak, T. Wojciechowski, M. Chudy, D. Moszczyńska, A. Wójcik, K. Prenger and M. Naguib, Juggling Surface Charges of 2D Niobium Carbide MXenes for a Reactive Oxygen Species Scavenging and Effective Targeting of the Malignant Melanoma Cell Cycle into Programmed Cell Death, *ACS Sustainable Chem. Eng.*, 2020, **8**(21), 7942–7951, DOI: [10.1021/acssuschemeng.0c01609](https://doi.org/10.1021/acssuschemeng.0c01609).
- 70 Y. Zhang, M. Li, X. Zhang, P. Zhang, Z. Liu, M. Feng, G. Ren and J. Liu, Tumor microenvironment-activated Nb<sub>2</sub>C quantum dots/lactate oxidase nanocatalyst mediates lactate consumption and macrophage repolarization for enhanced chemodynamic therapy, *Colloids Surf., B*, 2023, **221**, 113005, DOI: [10.1016/j.colsurfb.2022.113005](https://doi.org/10.1016/j.colsurfb.2022.113005).
- 71 X. Lin, Z. Li, S. Du, Q. Wang, Y. Guan, G. Cheng, H. Hong, J. Li, X. Chen and T. Chen, Occam's Razor-Inspired Nb<sub>2</sub>C



- delivery platform potentiates breast cancer therapy and inhibits lung metastasis, *Chem. Eng. J.*, 2023, **464**, 142732, DOI: [10.1016/j.cej.2023.142732](https://doi.org/10.1016/j.cej.2023.142732).
- 72 C. Du, W. Feng, X. Dai, J. Wang, D. Geng, X. Li, Y. Chen and J. Zhang, Cu<sup>2+</sup> + -Chelatable and ROS-Scavenging MXenzyme as NIR-II-Triggered Blood-Brain Barrier-Crossing Nanocatalyst against Alzheimer's Disease, *Small*, 2022, **18**(39), 2203031, DOI: [10.1002/smll.202203031](https://doi.org/10.1002/smll.202203031).
- 73 S. Wu, S. Du, Y. Guan, Q. Lin, Y. Liu, R. Lv, Z. Zhang, Y. Xia, T. Chen and H. Hong, V2C-Driven Nanodelivery Platform Potentiates Synergistic Breast Cancer Therapy, *ACS Mater. Lett.*, 2023, **5**(11), 3017–3031, DOI: [10.1021/acsmaterialslett.3c00965](https://doi.org/10.1021/acsmaterialslett.3c00965).
- 74 R. Zhao, Y. Zhu, L. Feng, B. Liu, Y. Hu, H. Zhu, Z. Zhao, H. Ding, S. Gai and P. Yang, Architecture of Vanadium-Based MXene Dysregulating Tumor Redox Homeostasis for Amplified Nanozyme Catalytic/Photothermal Therapy, *Adv. Mater.*, 2024, **36**(2), 2307115, DOI: [10.1002/adma.202307115](https://doi.org/10.1002/adma.202307115).
- 75 J. Deng, D. Xian, X. Cai, S. Liao, S. Lei, F. Han, Y. An, Q. He, G. Quan and C. Wu, *et al.*, Surface-Engineered Vanadium Carbide MXenzyme for Anti-Inflammation and Photoenhanced Antitumor Therapy of Colon Diseases, *Adv. Funct. Mater.*, 2023, **33**(31), 2211846, DOI: [10.1002/adfm.202211846](https://doi.org/10.1002/adfm.202211846).
- 76 Y. Cao, T. Wu, K. Zhang, X. Meng, W. Dai, D. Wang, H. Dong and X. Zhang, Engineered Exosome-Mediated Near-Infrared-II Region V2C Quantum Dot Delivery for Nucleus-Target Low-Temperature Photothermal Therapy, *ACS Nano*, 2019, **13**(2), 1499–1510, DOI: [10.1021/acsnano.8b07224](https://doi.org/10.1021/acsnano.8b07224).
- 77 A. Rafieerad, W. Yan, K. N. Alagarsamy, A. Srivastava, N. Sareen, R. C. Arora and S. Dhingra, Fabrication of Smart Tantalum Carbide MXene Quantum Dots with Intrinsic Immunomodulatory Properties for Treatment of Allograft Vasculopathy, *Adv. Funct. Mater.*, 2021, **31**(46), 2106786, DOI: [10.1002/adfm.202106786](https://doi.org/10.1002/adfm.202106786).
- 78 L. Wang, L. Zhuang, S. He, F. Tian, X. Yang, S. Guan, G. I. N. Waterhouse and S. Zhou, Nanocarbon Framework-Supported Ultrafine Mo<sub>2</sub>C@MoO<sub>x</sub> Nanoclusters for Photothermal-Enhanced Tumor-Specific Tandem Catalysis Therapy, *ACS Appl. Mater. Interfaces*, 2021, **13**(50), 59649–59661, DOI: [10.1021/acami.1c17085](https://doi.org/10.1021/acami.1c17085).
- 79 X. Ren, D. Chen, Y. Wang, H. Li, Y. Zhang, H. Chen, X. Li and M. Huo, Nanozymes-recent development and biomedical applications, *J. Nanobiotechnol.*, 2022, **20**(1), 92, DOI: [10.1186/s12951-022-01295-y](https://doi.org/10.1186/s12951-022-01295-y).
- 80 W. Feng, X. Han, H. Hu, M. Chang, L. Ding, H. Xiang, Y. Chen and Y. Li, 2D vanadium carbide MXenzyme to alleviate ROS-mediated inflammatory and neurodegenerative diseases, *Nat. Commun.*, 2021, **12**(1), 2203, DOI: [10.1038/s41467-021-22278-x](https://doi.org/10.1038/s41467-021-22278-x).
- 81 H. Yang, L. Xia, X. Ye, J. Xu, T. Liu, L. Wang, S. Zhang, W. Feng, D. Du and Y. Chen, Ultrathin Niobium Carbide MXenzyme for Remediating Hypertension by Antioxidative and Neuroprotective Actions, *Angew. Chem., Int. Ed.*, 2023, **62**(26), e202303539, DOI: [10.1002/anie.202303539](https://doi.org/10.1002/anie.202303539).
- 82 S. Irvani and R. S. Varma, MXene-Based Composites as Nanozymes in Biomedicine: A Perspective, *Nano-Micro Lett.*, 2022, **14**(1), 213, DOI: [10.1007/s40820-022-00958-7](https://doi.org/10.1007/s40820-022-00958-7).
- 83 V. S. Sivasankarapillai, A. K. Somakumar, J. Joseph, S. Nikazar, A. Rahdar and G. Z. Kyzas, Cancer theranostic applications of MXene nanomaterials: Recent updates, *Nano-Struct. Nano-Objects*, 2020, **22**, 100457, DOI: [10.1016/j.nanoso.2020.100457](https://doi.org/10.1016/j.nanoso.2020.100457).
- 84 Z. Liu, M. Zhao, L. Yu, W. Peng, Y. Chen and S. Zhang, Redox chemistry-enabled stepwise surface dual nanoparticle engineering of 2D MXenes for tumor-sensitive T1 and T2 MRI-guided photonic breast-cancer hyperthermia in the NIR-II biowindow, *Biomater. Sci.*, 2022, **10**(6), 1562–1574, DOI: [10.1039/D1BM01957K](https://doi.org/10.1039/D1BM01957K).
- 85 C. Dai, Y. Chen, X. Jing, L. Xiang, D. Yang, H. Lin, Z. Liu, X. Han and R. Wu, Two-Dimensional Tantalum Carbide (MXenes) Composite Nanosheets for Multiple Imaging-Guided Photothermal Tumor Ablation, *ACS Nano*, 2017, **11**(12), 12696–12712, DOI: [10.1021/acsnano.7b07241](https://doi.org/10.1021/acsnano.7b07241).
- 86 H. Lin, Y. Wang, S. Gao, Y. Chen and J. Shi, Theranostic 2D Tantalum Carbide (MXene), *Adv. Mater.*, 2018, **30**(4), 1703284, DOI: [10.1002/adma.201703284](https://doi.org/10.1002/adma.201703284).
- 87 C. Gokce, C. Gurcan, O. Besbinar, M. A. Unal and A. Yilmazer, Emerging 2D materials for antimicrobial applications in the pre- and post-pandemic era, *Nanoscale*, 2022, **14**(2), 239–249, DOI: [10.1039/D1NR06476B](https://doi.org/10.1039/D1NR06476B).
- 88 R. P. Pandey, P. A. Rasheed, T. Gomez, K. Rasool, J. Ponraj, K. Prenger, M. Naguib and K. A. Mahmoud, Effect of Sheet Size and Atomic Structure on the Antibacterial Activity of Nb-MXene Nanosheets, *ACS Appl. Nano Mater.*, 2020, **3**(11), 11372–11382, DOI: [10.1021/acsanm.0c02463](https://doi.org/10.1021/acsanm.0c02463).
- 89 A. Wojciechowska, M. Jakubczak, D. Moszczyńska, A. Wójcik, K. Prenger, M. Naguib and A. M. Jastrzębska, Engineering the surface of Nbn + 1CnTx MXenes to versatile bio-activity towards microorganisms, *Biomater. Adv.*, 2023, **153**, 213581, DOI: [10.1016/j.bioadv.2023.213581](https://doi.org/10.1016/j.bioadv.2023.213581).
- 90 C. Yang, Y. Luo, H. Lin, M. Ge, J. Shi and X. Zhang, Niobium Carbide MXene Augmented Medical Implant Elicits Bacterial Infection Elimination and Tissue Regeneration, *ACS Nano*, 2021, **15**(1), 1086–1099, DOI: [10.1021/acsnano.0c08045](https://doi.org/10.1021/acsnano.0c08045).
- 91 L. Ma, X. Zhang, H. Wang, X. Feng, J. Lei, Y. He, J. Wei, Y. Zhang, L. Tan and C. Yang, Two-dimensional Nb<sub>2</sub>C-based nanoplatform augmented sonodynamic antibacterial therapy and bone regeneration, *Sci. China Mater.*, 2023, **66**(7), 2913–2924, DOI: [10.1007/s40843-022-2413-4](https://doi.org/10.1007/s40843-022-2413-4).
- 92 Z. Yang, H. Zheng, H. Yin, L. Zhou, Q. Zhang and B. Zhang, Niobium carbide doped ROS/temperature dual-responsive multifunctional hydrogel for facilitating MRSA-infected wound healing, *Chem. Eng. J.*, 2023, **471**, 144634, DOI: [10.1016/j.cej.2023.144634](https://doi.org/10.1016/j.cej.2023.144634).
- 93 J. Chen, Y. Liu, G. Cheng, J. Guo, S. Du, J. Qiu, C. Wang, C. Li, X. Yang and T. Chen, *et al.*, Tailored Hydrogel Delivering Niobium Carbide Boosts ROS-Scavenging and Antimicrobial Activities for Diabetic Wound Healing, *Small*, 2022, **18**(27), 2201300, DOI: [10.1002/smll.202201300](https://doi.org/10.1002/smll.202201300).



- 94 H. Yuan, X. Hong, H. Ma, C. Fu, Y. Guan, W. Huang, J. Ma, P. Xia, M. Cao and L. Zheng, *et al.*, MXene-Based Dual Functional Nanocomposite with Photothermal Nanozyme Catalytic Activity to Fight Bacterial Infections, *ACS Mater. Lett.*, 2023, 5(3), 762–774, DOI: [10.1021/acsmaterialslett.2c00771](https://doi.org/10.1021/acsmaterialslett.2c00771).
- 95 L. Zong, Y. Yu, J. Wang, P. Liu, W. Feng, X. Dai, L. Chen, C. Gunawan, S. L. Jimmy Yun and R. Amal, *et al.*, Oxygen-vacancy-rich molybdenum carbide MXene nanonetworks for ultrasound-triggered and capturing-enhanced sonocatalytic bacteria eradication, *Biomaterials*, 2023, 296, 122074, DOI: [10.1016/j.biomaterials.2023.122074](https://doi.org/10.1016/j.biomaterials.2023.122074).
- 96 Q. Lv, Y. Zhou, L. Wang, S. Zhu, H. Lu, W. Yang and C. Wei, Mo<sub>2</sub>C nanosheets decorated with boron dipyrromethene enabling photothermal and photodynamic attributes for highly efficient antibacterials, *Appl. Surf. Sci.*, 2024, 652, 159216, DOI: [10.1016/j.apsusc.2023.159216](https://doi.org/10.1016/j.apsusc.2023.159216).
- 97 S. Zada, H. Lu, F. Yang, Y. Zhang, Y. Cheng, S. Tang, W. Wei, Y. Qiao, P. Fu and H. Dong, *et al.*, V<sub>2</sub>C Nanosheets as Dual-Functional Antibacterial Agents, *ACS Appl. Bio Mater.*, 2021, 4(5), 4215–4223, DOI: [10.1021/acsubm.1c00008](https://doi.org/10.1021/acsubm.1c00008).
- 98 W. Zhao, L. Jiang, H. Yang, Z. Yu, Z. Yang and Y. Zhou, Antibacterial effect and photothermal sterilization of low dose two-dimensional vanadium carbide, *Appl. Phys. A: Mater. Sci. Process.*, 2023, 129(4), 308, DOI: [10.1007/s00339-023-06602-4](https://doi.org/10.1007/s00339-023-06602-4).
- 99 X. Feng, D. Xian, J. Fu, R. Luo, W. Wang, Y. Zheng, Q. He, Z. Ouyang, S. Fang and W. Zhang, *et al.*, Four-armed host-defense peptidomimetics-augmented vanadium carbide MXene-based microneedle array for efficient photo-excited bacteria-killing, *Chem. Eng. J.*, 2023, 456, 141121, DOI: [10.1016/j.cej.2022.141121](https://doi.org/10.1016/j.cej.2022.141121).
- 100 M. Lian, Y. Zhao, J. Zhao, W. Zhang, H. Zhang and D. Chen, Oxidase-like V<sub>2</sub>C MXene nanozyme with inherent antibacterial properties for colorimetric sensing, *Talanta*, 2023, 265, 124872, DOI: [10.1016/j.talanta.2023.124872](https://doi.org/10.1016/j.talanta.2023.124872).
- 101 J.-H. Ahn, M.-J. Lee, H. Heo, J. H. Sung, K. Kim, H. Hwang and M.-H. Jo, Deterministic Two-Dimensional Polymorphism Growth of Hexagonal n-Type SnS<sub>2</sub> and Orthorhombic p-Type SnS Crystals, *Nano Lett.*, 2015, 15(6), 3703–3708, DOI: [10.1021/acs.nanolett.5b00079](https://doi.org/10.1021/acs.nanolett.5b00079).
- 102 X. Sun, X. He, Y. Zhu, E. Obeng, B. Zeng, H. Deng, J. Shen and R. Hu, Valence-switchable and biocatalytic vanadium-based MXene nanoplatform with photothermal-enhanced dual enzyme-like activities for anti-infective therapy, *Chem. Eng. J.*, 2023, 451, 138985, DOI: [10.1016/j.cej.2022.138985](https://doi.org/10.1016/j.cej.2022.138985).
- 103 Q. He, H. Hu, J. Han and Z. Zhao, Double transition-metal TiVCTX MXene with dual-functional antibacterial capability, *Mater. Lett.*, 2022, 308, 131100, DOI: [10.1016/j.matlet.2021.131100](https://doi.org/10.1016/j.matlet.2021.131100).
- 104 M. Khazaei, A. Ranjbar, M. Arai, T. Sasaki and S. Yunoki, Electronic properties and applications of MXenes: a theoretical review, *J. Mater. Chem. C*, 2017, 5(10), 2488–2503, DOI: [10.1039/C7TC00140A](https://doi.org/10.1039/C7TC00140A).
- 105 K. Rajavel, S. Shen, T. Ke and D. Lin, Achieving high bactericidal and antibiofouling activities of 2D titanium carbide (Ti<sub>3</sub>C<sub>2</sub>T<sub>x</sub>) by delamination and intercalation, *2D Mater.*, 2019, 6(3), 035040, DOI: [10.1088/2053-1583/ab23ce](https://doi.org/10.1088/2053-1583/ab23ce).
- 106 D. Wu, R. Zhao, Y. Chen, Y. Wang, J. Li and Y. Fan, Molecular insights into MXene destructing the cell membrane as a “nano thermal blade”, *Phys. Chem. Chem. Phys.*, 2021, 23(5), 3341–3350.
- 107 S. Venkateshalu, M. Shariq, B. Kim, M. Patel, K. S. Mahabari, S.-I. Choi, N. K. Chaudhari, A. N. Grace and K. Lee, Recent advances in MXenes: beyond Ti-only systems, *J. Mater. Chem. A*, 2023, 11(25), 13107–13132, DOI: [10.1039/D3TA01590D](https://doi.org/10.1039/D3TA01590D).

